Virology 526 (2019) 189–202

Contents lists available at ScienceDirect

Virology

journal homepage: www.elsevier.com/locate/virology

Variable infectivity and conserved engagement in cell-to-cell viral transfer by HIV-1 Env from Clade B transmitted founder clones

Hongru Li, Benjamin K. Chen*

Division of Infectious Disease, Department of Medicine, Immunology Institute, Icahn School of Medicine at Mount Sinai, New York, NY 10029, United States

ARTICLE INFO

Keywords:
Human immunodeficiency virus type 1 (HIV-1)
Envelope (Env)
Transmitted/ founder (T/F)
Cell-free infection
Cell-to-cell infection
Virological synapses (VS)
Cell-to-cell transfer
Fusogenicity

ABSTRACT

HIV-1 transmission is usually initiated by a single viral strain called transmitted/ founder (T/F) virus. In *in vitro* models, HIV-1 can efficiently spread via cell-free and virological synapse (VS)-mediated cell-to-cell infection. Both modes of infection require the viral glycoprotein Envelope (Env). The efficiency with which T/F Envs initiate VS and mediate cell-to-cell infection has not been well characterized. Here we tested a panel of isogenic HIV-1 molecular clones that carry different Clade B T/F Envs. We found that despite variable infectivity among different Env clones in the two modes of infection, T/F Envs generally mediated efficient VS formation and subsequent cell-to-cell transfer. In contrast, *in vitro* infectivity of the T/F Env clones was more variable and strongly correlated with intrinsic fusogenicity of various Envs. We speculate that the conservation of cell-to-cell transfer by T/F Env is indicative of a biologically important function of Env.

1. Introduction

HIV-1 glycoprotein Envelope (Env) is a viral protein expressed on HIV-1 virions as well as the surface of HIV-1 infected cells. It is responsible for mediating viral attachment to CD4 receptors on target cells and driving viral membrane fusion (Wyatt and Sodroski, 1998). As the only surface viral protein, it is also the target of neutralizing antibodies that can block the spread of the virus. HIV-1 Env is synthesized as a 160kD precursor glycoprotein, gp160, which is subsequently enzymatically cleaved into two non-covalently bound subunits, gp120 and gp41 (Hallenberger et al., 1992). The surface subunit (SU) gp120 is the receptor binding protein. Its interaction with the CD4 receptor triggers the membrane fusion reaction (Hunter and Swanstrom, 1990; Freed and Martin, 1995). The trans-membrane (TM) subunit gp41 has an ~150 amino-acid-long cytoplasmic tail, which serves several important functions, including: cellular trafficking of Env, directing polarized budding of virus particles, incorporation of Env into virus particles, regulation of viral fusion, and endocytosis of Env. Trimers of gp120/ gp41 heterodimer form the Env spike structure, which HIV-1 is completely dependent upon for host cell entry and HIV-1 infection (Wyatt and Sodroski, 1998; Freed and Martin, 1995; Checkley et al., 2011).

HIV-1 infection can be initiated by both cell-free and cell-associated virus. Cell-free infection occurs when free HIV-1 particles are released from infected cells, and proceed to infect non-adjacent, uninfected $CD4^+$ T cells. It provides a mechanism of viral dissemination to uninfected $CD4^+$ T cells at a distance via lymphatic flow or blood circulation. In contrast, cell-to-cell infection is mediated by direct adhesive cell-cell contact structures that form between HIV-1 infected and uninfected $CD4^+$ T cells. This direct adhesive connection is called the virological synapse (VS). The T cell VS has been characterized as an actin-dependent polarization of viral proteins Env and Gag on the infected cells and CD4 receptors that are recruited on uninfected target cells to the cell-to-cell contact region (Jolly et al., 2004). Interactions between intercellular adhesion molecules (ICAM) 1 and 3 and LFA-1 may further stabilize the VS (Jolly et al., 2007; Jolly and Sattentau, 2004). Cell-to-cell infection is found to be much more efficient *in vitro* compared to cell-free infection (Chen et al., 2007; Sourisseau et al., 2007) and enables the virus to resist certain classes of antiviral drugs (Sigal et al., 2011; Titanji et al., 2013) as well as broadly neutralizing antibodies (bNAbs) in an epitope- and viral strain-dependent manner (Reh et al., 2015; Li et al., 2017).

Previous studies from our group and others support a model of cell-to-cell transmission, whereby HIV-1 initially transfers across the VS in a co-receptor independent manner into trypsin-resistant endocytic compartments within the HIV-1 uninfected target $CD4^+$ T cells (Chen et al., 2007; Dale et al., 2011; Bosch et al., 2008; Sloan et al., 2013). Subsequent viral fusion requires viral protease (PR)-dependent cleavage of viral protein Gag and maturation of the virus from within the target cell

* Correspondence to: Division of Infectious Disease, Department of Medicine, Icahn School of Medicine at Mount Sinai, One Gustave Levy Place, Box 1090, New York, NY 10029, United States.
E-mail addresses: hongru.li@mssm.edu (H. Li), ben.chen@mssm.edu (B.K. Chen).

https://doi.org/10.1016/j.virol.2018.10.016
Received 4 August 2018; Received in revised form 16 October 2018; Accepted 16 October 2018
Available online 08 November 2018
0042-6822/

(Dale et al., 2011). Time-lapse live imaging studies suggest that interactions between Env and CD4 occur prior to the recruitment of Gag to the cell-cell contact region (Hubner et al., 2009), indicating that Env initially functions as an adhesion molecule during formation of VS (Chen, 2012). Viral fusion events within endocytic compartments of individual target cells have also been observed (Dale et al., 2011). Previous studies in humanized mice, non-human primates and *ex vivo* human explants implicate cell-associated HIV-1 and SIV-1 in systemic viral dissemination (Murooka et al., 2012) and mucosal transmission (Kolodkin-Gal et al., 2013; Bernard-Stoecklin et al., 2014). Although the extent to which cell-to-cell infection of HIV-1 occurs *in vivo* remains uncertain, recent studies indicate that cell-to-cell infection is operative *in vivo* in humanized mice, especially in the $CD4^+$ cell-dense lymphoid tissues (Law et al., 2016).

Chronically HIV-1-infected individuals typically harbor very diverse HIV-1 populations in their blood. However, during acute mucosal transmission, viral diversity within donors is severely reduced through a genetic bottleneck. Acute HIV-1 infection is mostly initiated with a single viral strain or, in rare cases, more than one closely related strain called transmitted / founder (T/F) viruses (Keele et al., 2008; Salazar-Gonzalez et al., 2008; Keele, 2010; Keele and Derdeyn, 2009). T/F viruses are initially homogeneous during acute infection and diversify over time by accumulating errors from reverse transcriptase, Pol II, or innate cellular cytosine deaminases APOBEC 3 (Keele et al., 2008; Keele and Derdeyn, 2009; Learn et al., 2002). Investigators have been interested in understanding phenotypic properties of T/F Envs that are associated with viral transmission. T/F Envs can be distinguished from chronic viruses by their co-receptor utilization (Parker et al., 2013; Ashokkumar et al., 2018). T/F viruses of different subtypes display differential preference for CD4/CCR5 expression levels during viral entry (Chikere et al., 2014). T/F viruses have also been reported to be more infectious (Ashokkumar et al., 2018; Parrish et al., 2013) and to package 1.9-fold more Env per particle compared to chronic viruses (Parrish et al., 2013). They also display enhanced dendritic cell interactions and increased resistance to type 1 interferon (IFN) over chronic control viruses (Parrish et al., 2013; Iyer et al., 2017; Fenton-May et al., 2013). This resistance to IFN is thought to be mediated by resistance to IFN induced trans-membrane proteins (IFITMs) (Foster et al., 2016; Wang et al., 2017; Yu et al., 2015), which have been shown to antagonize Env protein and alter infection in both cell-free and cell-to-cell routes (Foster et al., 2016; Yu et al., 2015). Other studies suggest that T/F variants do not inherently replicate faster than related non-transmitted viruses from the same donor near the estimated time of transmission regardless of type 1 IFN (Deymier et al., 2015). Interestingly, mutants that escaped from adaptive immune response were found to become less resistant to IFN, and tend to reduce their transmission potential (Foster et al., 2016). Another report from Oberle et al. observed that T/F viruses were more sensitive to INF compared to non-transmitted viruses from the same HIV-1- infected donor, while no other phenotypic properties were observed including cell-to-cell transmission efficiency, replicative capacity, entry kinetics and sensitivity to entry inhibitors and neutralizing antibodies (Oberle et al., 2016).

Previous studies have also identified the degree of occupancy of potential N-linked glycosylation sites (PNGS) and found that T/F Envs possess fewer PNGS and shorter variable loops (V1V2) compared to chronic Envs from the same infected individual (Derdeyn et al., 2004; Chohan et al., 2005; Li et al., 2006; Liu et al., 2008; Go et al., 2011). While shorter V1V2 and fewer PNGS have generally been associated with greater sensitivity to antibody neutralization (Derdeyn et al., 2004; Back et al., 1994; Cao et al., 1997; Koch et al., 2003; Ly and Stamatatos, 2000; McCaffrey et al., 2004; Stamatatos and Cheng-Mayer, 1998; Reitter et al., 1998), there are conflicting reports on the neutralization susceptibility of T/F viruses versus corresponding chronic viruses (Hraber et al., 2014; Ping et al., 2013; Wilen et al., 2011; Frost et al., 2005).

Previous studies of T/F Envs in the context of either infectious molecular clones or isogenic wild type proviral clones have mostly focused on cell-free infection. Characterization of HIV-1 T/F Envs in cell-to-cell transmission remains limited (Reh et al., 2015; Li et al., 2017; Oberle et al., 2016; Abela et al., 2012; Malbec et al., 2013; Brandenberg et al., 2014; Gombos et al., 2015). In this study, we constructed a panel of fluorescent protein-expressing, replication-competent HIV-1 proviral molecular clones that express T/F Envs, and established flow cytometry-based assays to follow cell-to-cell transfer and subsequent viral fusion in T cell lines during HIV-1 cell-to-cell transmission. This panel of T/F Envs is geographically and genetically diverse clade B viral isolates (Table 1). We examined their infectivity in cell-free as well as cell-to-cell infection, and observed strong correlation of infectivity in the two modes of infection. Different T/F Envs exhibited a broad range of relative infectivity that significantly correlated with Env fusogenicity, while remaining similar in their ability to initiate VS-mediated transfer of virus between infected and uninfected $CD4^+$ T cells. This panel of T/F Envs-expressing proviral molecular clones provides a valuable Clade B reference panel to characterize T/F Envs and to study their neutralization sensitivity against bNAbs with high sensitivity and wide dynamics.

Table 1
Reference panel for Clade B HIV-1 T/F Env clones.

Env clone name	Reagent Contributor[1]	Accession number	Origin	Tier	Subtype
6535.3	A	AY835438	Washington DC	1B	B
QH0692	A	AY835439	Trinidad	2	B
PVO4	A	AY835444	Italy	3	B
WITO	B	AY835451	Alabama	2	B
REJO	B	AY835449	Alabama	2	B
RHPA	B	AY835447	Tennessee	2	B
SC422661	A	AY835441	Trinidad	2	B

Contributors[1]
A- Drs. David Montefiore, Feng Gao and Ming Li.
B- Drs. B. H. Hahn and J. F. Salazar-Gonzalez.

2. Results

2.1. Characterization of fluorescent protein-expressing proviral molecular constructs with T/F Envs

To characterize infection efficiency of HIV-1 T/F viruses in cell-free and cell-to-cell transmission, a panel of genetically and geographically diverse full-length Clade B T/F Envs (ARP, Table 1) was cloned into a previously described NL4-3 based fluorescent protein-expressing replication competent proviral molecular clone NLCI (Li et al., 2017; Cohen et al., 1999), substituting NL4-3 Env. These genetically and geographically diverse Envs were initially isolated from patients at different Fiebig stages (Fiebig et al., 2003) during acute infection, representing the majority of currently circulating viral strains in North America. They displayed diverse neutralization sensitivities when pseudotyped with *env*-deficient HIV-1 backbone, as measured by standard TZM-bl assay (Seaman et al., 2010). Since the panel of T/F Envs is all R-tropic, $NLCI_{JRFL}$ was generated similarly as the R-tropic chronic virus control. These viral constructs allowed us to compare the infectivity of cell-free versus cell-associated infection, where the only differences among the clones are in the Env glycoprotein.

When transfecting 293T cells, all the viral constructs efficiently expressed Envs as demonstrated by Western Blot of cell lysates of transfected 293T cells (Fig. 1A). Viral production efficiency of T/F constructs was comparable to wild type $NLCI_{NL4-3}$ (Fig. 1B). To determine if T/F Envs can be efficiently incorporated into virus particles, Western Blot with lysed virus particles was performed (Fig. 1C). Quantitation of Western Blots of lysed virus particles showed that Env incorporation into chimeric constructs carrying T/F Envs or JRFL Env

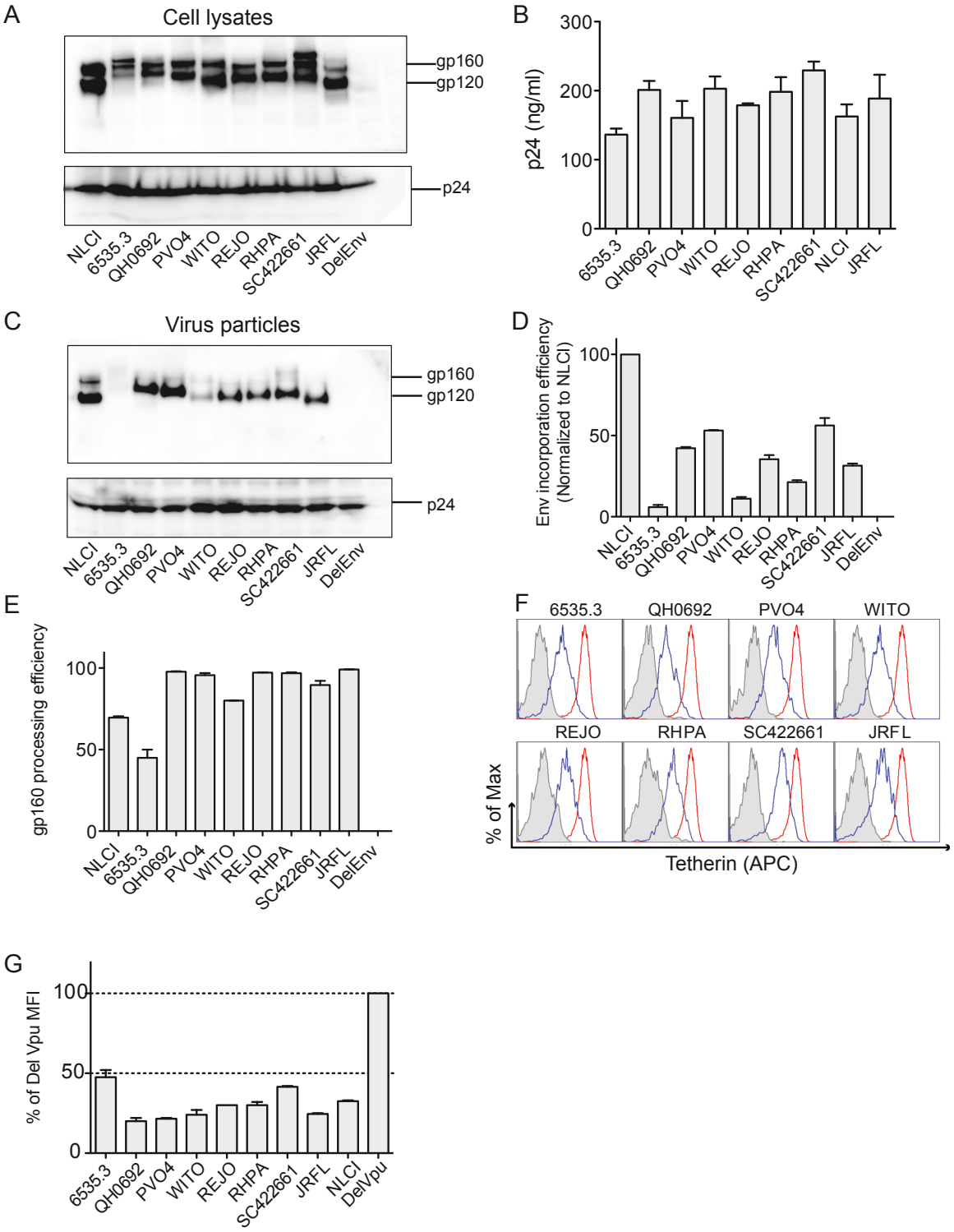

Fig. 1. T/F Env-chimeric viral genomes preserve intact virus production and Env incorporation. (A) T/F Envs expression in transfected 293T cells by Western Blot. (B) Viral production from 293T cells transfected with NLCI constructs bearing different Envs was quantitated by p24 ELISA. (C) Env incorporation into viral particles was examined by Western Blot. The amount of sample loaded was normalized to the sample p24 content. (D) Quantitation of Western Blots for Env incorporation efficiency into virus particles. (E) Quantitation of Western Blots for Env processing efficiency from gp160 precursor to gp120. (F) Vpu activity was assessed by measuring down modulation of surface Tetherin expression on Tetherin^{high} Jurkat cells nucleofected with T/F constructs. Gray shaded histogram represents a non-stained control. Dashed black histogram shows the Tetherin expression level in each sample and solid black line showed Vpu deficient virus control. (G) Quantitation of Tetherin down modulation compared to ΔVpu construct. (For interpretation of the references to color in this figure legend, the reader is referred to the web version of this article.).

was lower compared to $NLCI_{NL4-3}$ (Fig. 1D). WITO Env incorporation efficiency was much lower than others and 6535.3 Env was packaged into virus particles at very low level (Figs. 1C and 1D). The majority of the gp160 precursors were processed into gp120, with efficiency comparable to wild type $NLCI_{NL4-3}$ (Fig. 1E).

Because of overlapping open reading frames in *env* and other viral genes, the panel of constructs with T/F Envs contains chimeric *tat, rev* and *vpu.* The robust production of cell-free virus indicates that *tat* and *rev* are functionally intact in these chimeric viruses. One primary function of HIV-1 Vpu is to down-modulate Tetherin expression on the surface of HIV-1-infected cells. Chimeric *vpu* generated in these clones was found to be capable of down-modulating cell-surface Tetherin expression in Tetherin-high Jurkat cells by 2–4-fold compared to NLCI-ΔVpu (Alvarez et al., 2014), to a level comparable to the parental $NLCI_{NL4-3}$ construct (Fig. 1F,G). This suggested that chimeric *vpu* in T/F Env constructs was still functional.

2.2. Infectivity of T/F viruses in TZM-bl assays

The infectivity of the viral clones was first measured by a single-round infection using the TZM-bl reporter cell line. Virus produced by transfecting 293T cells was used to infect TZM-bl cells in the presence and absence of 30 μg/ml DEAE-Dextran. The polycationic polymer, DEAE-Dextran, is thought to enhance adsorption of virions onto the cell surface and enhance viral infectivity by neutralizing charge repulsion between cell-free virus particles and cell-surface sialic acid (Konopka et al., 1991). We observed that T/F viruses displayed a wide range of infectivity and that they were about 5–96-fold less infectious than lab-adapted strain NL4-3 and chronic viral strain $NLCI_{JRFL}$ (Fig. 2A). Cell-free infection of the T/F viruses was significantly increased in the presence of DEAE-Dextran (Fig. 2A, C). Cell-to-cell infection assay was performed by co-culturing HIV-1 expressing donor cells and pre-seeded TZM-bl cells with and without the presence of DEAE-Dextran (Fig. 2B). Acutely nucleofected Jurkat cells with NLCI constructs were utilized as HIV-1 expressing donor cells as previously described (Li et al., 2017; Durham and Chen, 2016). In contrast to cell-free infection, cell-to-cell infection of TZM-bl cells was not as responsive to DEAE-Dextran treatment (Fig. 2B, C).

2.3. Infectivity of T/F viruses in single round cell-free and cell-to-cell infections

While the TZM-bl reporter assay is a useful indicator of infection, epithelial cells are not natural targets of HIV-1. To assess their infectivity in physiologically relevant T cell lines, we utilized sensitive, flow cytometry-based, single-round cell-free and cell-to-cell infection assays. Cell-free infection assays were performed by mixing cell-free virus with CCR5-expressing T cells. In cell-to-cell infection, HIV-1-nucleofected Jurkat cells were used as donor cells, and a CCR5-expressing T cell line served as target cells, as previously described (Li et al., 2017; Durham and Chen, 2016).

Several CCR5-expressing T cell lines including MT4R5, CEM.NKR.CCR5, Molt4.CCR5 and A3.01.CCR5 were used as target cells in both cell-free and VS-mediated cell-to-cell infection assays. Transfected 293T cell-produced T/F Env-expressing viruses exhibited a broad range of infectivity in both cell-free (Fig. 3A) and cell-to-cell infection in MT4R5 cells (Fig. 3B). CEM.NKR.CCR5 cells showed similar infection levels as the MT4R5 cells in cell-free infection route when a minimum of 16 μg/ml polybrene was present. A3.01.CCR5 cells were less infected, and Molt4.CCR5 cells were poorly infected (data not shown). In infection assays using T cell lines, lab-adapted strains and virus with T/F Env were normalized to the same amount of cell-free viral antigen or percentage of infected donor cells. We observed that viruses with T/F Envs were generally much less infectious, when challenged with comparable levels of viral antigen or infected cells, in comparison to lab-adapted strain $NLCI_{NL4-3}$ or chronic clone $NLCI_{JRFL}$ in all cell lines tested (Fig. 3A and B).

2.4. Recombinant viruses with T/F Envs are capable of multiple rounds of infection

To investigate if the viruses were capable of productive infection, we also performed multiple-round infection assays using PHA-activated primary $CD4^+$ T cells. Viruses with the same amount of p24 were used as cell-free inoculum (Fig. 4A) and nucleofected Jurkat cells with comparable levels of nucleofection efficiency were used as cell-associated inoculum (Fig. 4B). Samples were collected every two days post infection. The percentage of infection in primary $CD4^+$ T cells increased over time and plateaued at approximately four 4 days after infection, indicating that all viruses except clone 6535.3 were capable of multiple rounds of productive infection.

2.5. Viruses with T/F Envs are capable of efficient cell-to-cell transfer

Previous studies from our group and others suggested that during VS-mediated cell-to-cell transmission, HIV-1 is initially transferred

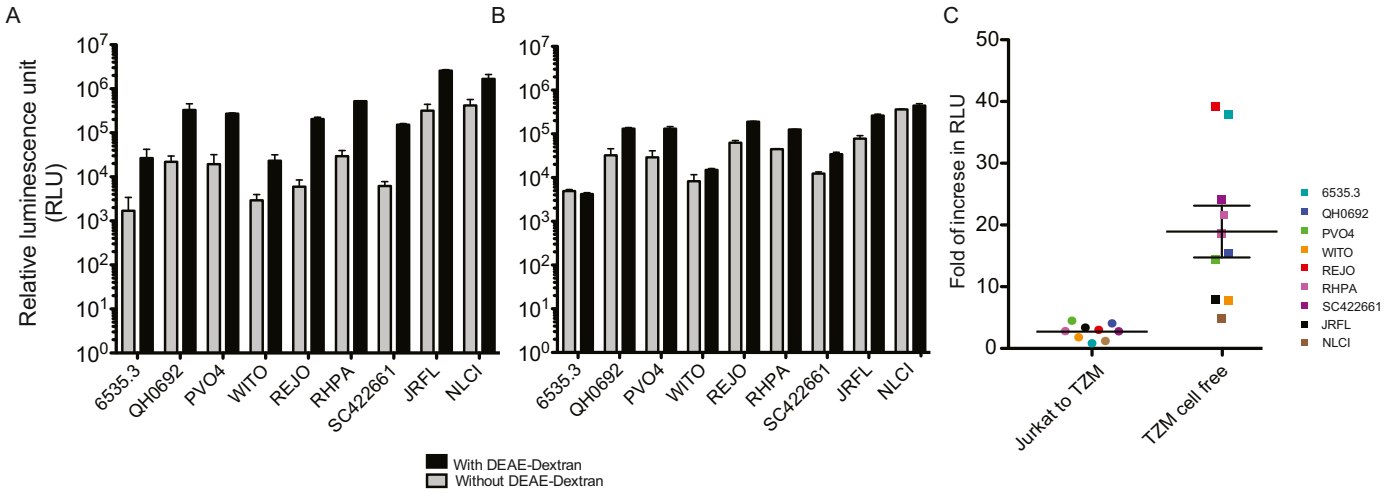

Fig. 2. Infectivity of viruses with T/F Envs in TZM-bl cells. (A) Infectivity of viruses was measured by of TZM-bl reporter cells in the presence and absence of 30 μg/ml DEAE-Dextran. Viral input was all normalized to 4.5 ng/well. (B) Cell-to-cell infection from HIV-1 expressing Jurkat donor cells to TZM-bl cell with and without the presence of DEAE-Dextran. Viral input was normalized to comparable level of nucleofection in Jurkat cells. (C) The effect of DEAE-Dextran on infection of TZM-bl cells by co-culture with nucleofected Jurkat cells expressing HIV-1 carrying T/F Envs, or by cell-free viruses.

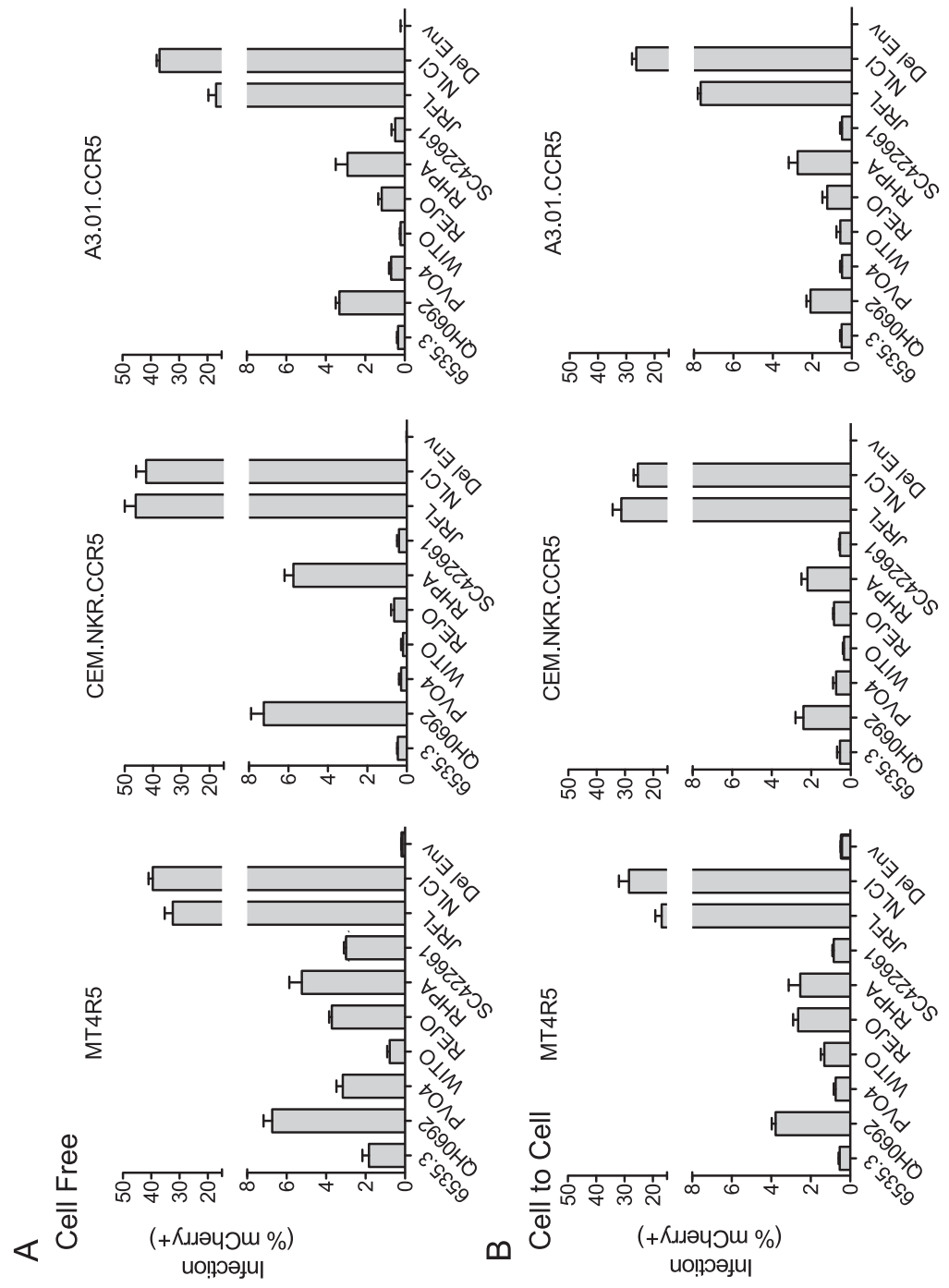

Fig. 3. Single round infectivity of viruses with T/F Envs in different T cell lines. (A) Single round cell-free infection levels of MT4R5 cells (left, 2 μg/ml polybrene present), CEM.NKR.CCR5 cells (middle, 16 μg/ml polybrene present), and A3.01.CCR5 cells (right, 2 μg/ml polybrene present) by 4 ng/well viruses with T/F Envs. Error bars represent the SEMs from duplicates of two independent experiments. (B) Single round cell-to-cell infection levels of MT4R5 cells (left), CEM.NKR.CCR5 cells (middle) and A3.01.CCR5 cells (right) after co-culture with nucleofected Jurkat donor cells expressing HIV-1 with T/F Envs. Error bars represent the SEMs from duplicates of two independent experiments.

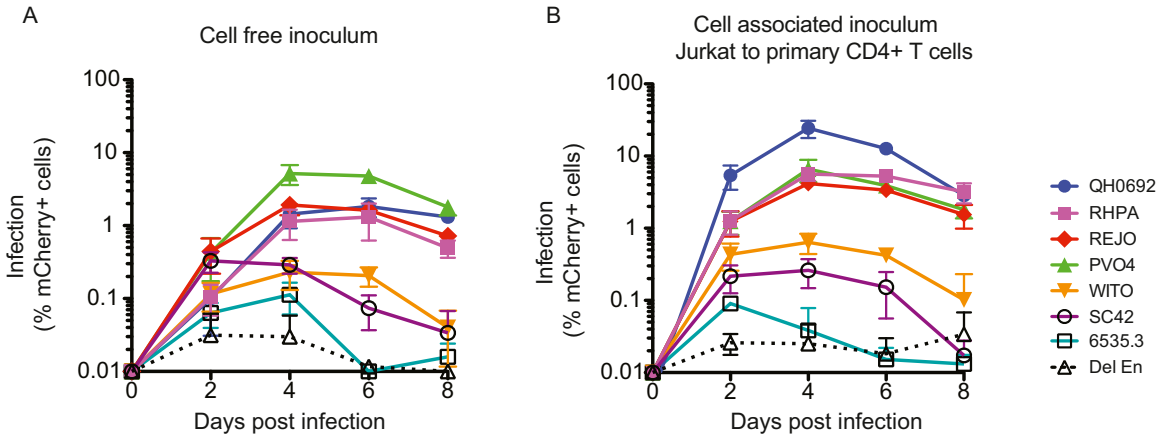

Fig. 4. Multi-round infectivity of HIV-1 carrying T/F Envs in primary CD4 + T cells. (A) Multi-round infection of activated primary CD4 + T cells initiated with transfected 293T cells produced cell-free viruses. (B) Multi-round infection of activated primary CD4 + T cells initiated by co-culturing with nucleofected Jurkat donor cells expressing HIV-1 that carry T/F Envs.

across Env-CD4 dependent VS in a co-receptor independent manner into trypsin-resistant endocytic compartments, followed by viral fusion in response to viral maturation induced by cleavage of Gag by PR with delayed kinetics (Chen et al., 2007; Dale et al., 2011; Hubner et al., 2009). Based on this two-step entry model, we proceeded to characterize cell-to-cell infection of T/F viruses by examining the efficiency of these viruses to transfer through VS from donor to target cells.

As the expression level of Env on the surface of HIV-1 infected cells may influence the efficiency of cell-to-cell infection, we first measured Env on the surface of HIV-1 expressing cells by antibody staining. T/F Envs were detected on the surface of Amaxa-nucleofected Jurkat cells by staining with the glycan-detecting monoclonal antibody 2G12 (Fig. 5A, B). REJO and RHPA were non-reactive with the 2G12. In contrast to the 2G12 staining, pooled HIV-1$^+$ patient IgG, VRC01 or b12 stained cells expressing the T/F clones weakly (data not shown).

We then assessed the ability of the viral clones to engage in formation of VS and cell-to-cell viral transfer. The panel of T/F Envs was cloned into fluorescent virus clone HIV-1 Gag-iGFP (Hubner et al., 2007), where GFP was inserted between MA and CA in frame, providing a sensitive fluorescent marker to indicate viral transfer between infected and uninfected cells. We used nucleofected Jurkat cells as donor cells and MT4R5 or CEM.NKR.CCR5 cells as target cells and performed the cell-to-cell transfer assay (Durham and Chen, 2016). Donor cells were normalized to the similar nucleofection efficiency by adjusting the amount of DNA in the nucleofection, or by diluting with un-transfected Jurkat cells. We found that the whole panel of T/F Envs displayed relatively comparable level of cell-to-cell transfer from nucleofected Jurkat cells to MT4R5 cells (Fig. 5C) and CEM.NKR.CCR5 cells (Fig. 5D), suggesting that the ability to engage in cell-to-cell transfer is similar among different T/F Envs. Surprisingly, even the poorly infectious clone 6535.3 was able to transfer at levels comparable with the more infectious clone QH0692. We note that the cell-to-cell transfer efficiency of Gag-iGFP-JRFL is still significantly higher than that observed in T/F constructs. However, the magnitude of difference in transfer efficiency between Gag-iGFP-JRFL and T/F constructs was about 4.6–26-fold lower than the difference observed in cell-to-cell infectivity with $NLCI_{JRFL}$ relative to corresponding T/F Envs expressing constructs in CEM.NKR.CCR5 cells and as much as 5-fold lower in MT4R5 cells. Taken together, these results suggest that each T/F Env achieves sufficient cell-surface Env expression to mediate -similar and efficient synapse formation and cell-to-cell transfer of HIV-1.

2.6. Correlation of cell-free infectivity and cell-to-cell infectivity

When the relative infection efficiencies of cell-free infection and that of cell-to-cell infection were plotted against each other, we observed that the relative infection efficiencies of the two modes of infection were significantly correlated (Fig. 6A, B). Interestingly, the T/F Envs generally possessed comparable abilities to initiate formation of VS and transfer of HIV-1 from donor to target cells. A significant correlation was not observed between the efficiency of cell-to-cell transfer and cell-to-cell infection (Fig. 6C, D). The results presented suggest that the fusion step that follows cell-to-cell transfer is likely to be the rate-limiting step influencing the infectivity of various T/F Envs.

2.7. Env fusogenicity significantly correlated with viral infectivity in vitro

To directly measure fusogenicity of T/F Envs in cell-free and viral fusion after cell-to-cell transfer step, we employed a Cre-lox-mediated viral membrane fusion assay (Esposito et al., 2016). We generated an indicator cell line that expresses a Cre-lox-activated genetic switch measuring the efficiency of Cre enzyme that is delivered to the target cell via viral membrane fusion of HIV-1 that packages large amounts of the Cre recombinase (Esposito et al., 2016). A3.01.CCR5 RG cell line was generated by transduction with a retroviral vector containing the red-to-green switch cassette, in which dsRed was flanked by a pair of LoxP and followed by eGFP (Fig. 7A) (Esposito et al., 2016). We subcloned the panel of T/F Envs Gag-iCre construct, in which Cre is inserted in frame between MA and CA, preserving the protease cleavage sites (Esposito et al., 2016). Upon viral fusion, Cre recombinase that was delivered from cell-free or cell-to-cell infection is introduced into target cells, bearing the Cre-sensitive genetic switch, thereby triggering a genetically encoded red-to-green color change (Fig. 7A). The percentage of GFP-positive cells within target population provides a measure of viral membrane fusion following the addition of a similar input of cell-free or cell-associated virus (Esposito et al., 2016). The relative abundance of GFP positive cells in target cells among different samples serves as a quantitative measure of the relative fusogenicity of each T/F Env. Env fusogenicity was measured in both cell-free virus particles (Fig. 7B) as well as in cell-associated virus (Fig. 7C). When Env fusogenicity was plotted against the relative infection efficiencies in cell-free and cell-to-cell infections, we observed that the relative infection efficiency correlated with Env fusogenicity in both routes of infection (Fig. 7D, E). When Env fusogenicity was plotted against its cell-to-cell transfer efficiency, no significant correlation was observed

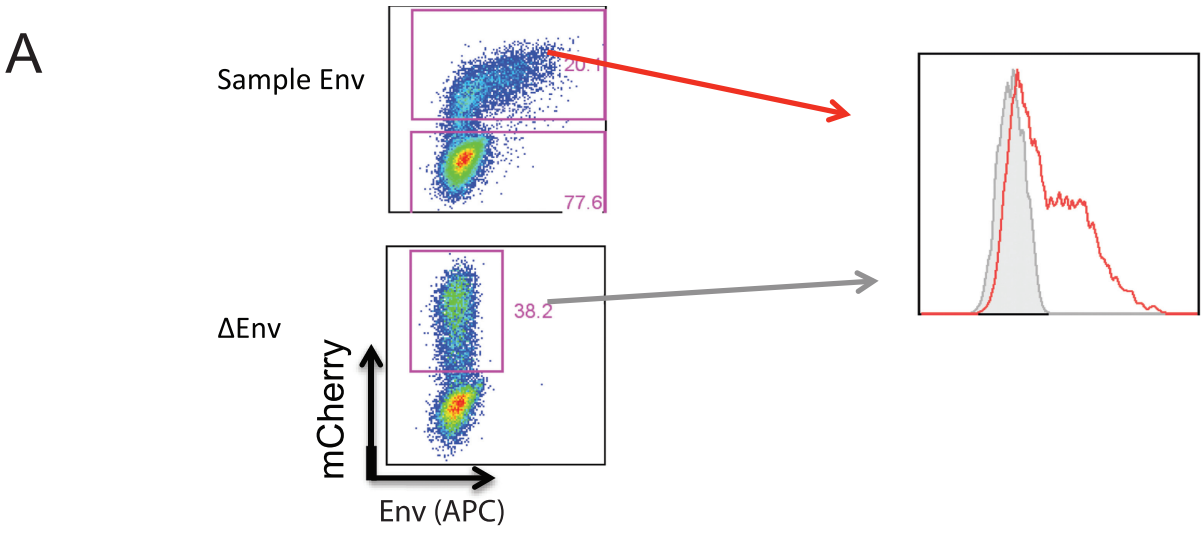

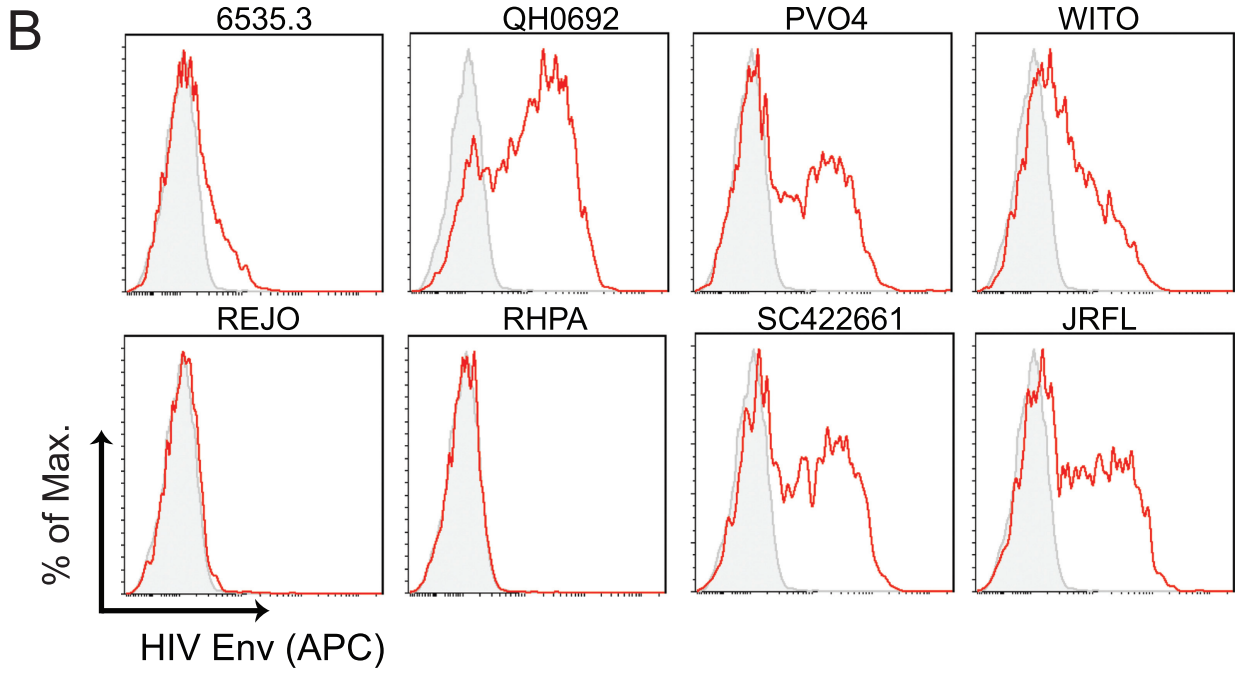

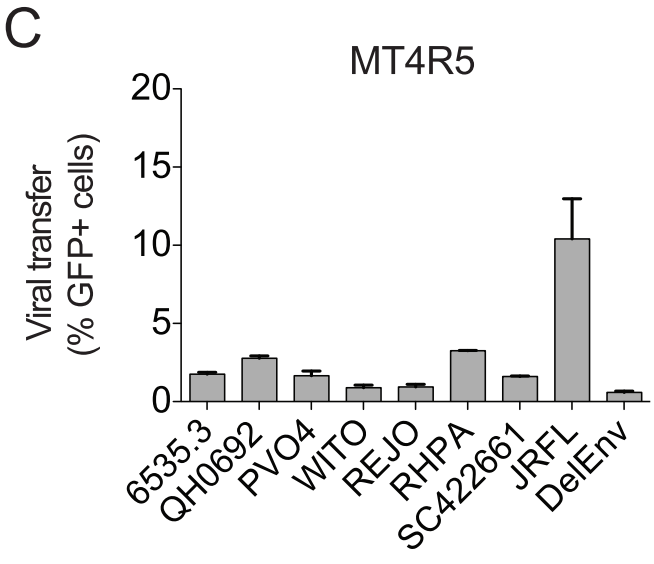

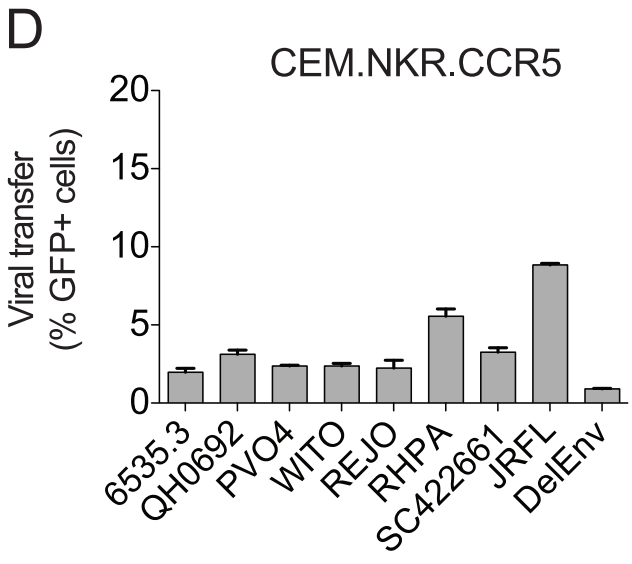

(caption on next page)

Fig. 5. HIV-1 with T/F Envs preserved efficient cell-to-cell transfer. (A) Representative flow cytometry plot and histogram of cell surface HIV-1 Env on Jurkat cells expressing HIV-1 with different Envs (red line) compared with Δenv (filled gray). (B) Different Envs were detected on Jurkat donor cells expressing high levels of HIV-1 (indicated by mCherry expression level) with mAb 2G12. (C) Cell-to-cell transfer levels of MT4R5 cells and (D) CEM.NKR.CCR5 cells after co-culturing with nucleofected Jurkat cells expressing HIV-1 with T/F Envs. Error bars represent SEMs of duplicates from two independent experiments. (For interpretation of the references to color in this figure legend, the reader is referred to the web version of this article.).

(Fig. 7F). These results suggest that the low infectivity of viruses carrying T/F Envs compared to lab-adapted virus is attributable to the intrinsically lower fusogenicity of T/F Envs. In our *in vitro* model, it is the intrinsic fusogenic potential of T/F Envs that ultimately determines cell-to-cell infectivity.

Since these recombinant viral clones pair a T/F Env with NL4-3 molecular backbone, it is possible that incompatibility of the Env with the NL4-3 backbone may affect early events of viral infection up to the point of viral gene expression. To determine if complementation of low fusogenicity of T/F Envs in viral entry would rescue the defects in infectivity of T/F viruses, we pseudotyped the NLCI constructs with VSV-G. We infected $CD4^-$ A2.01 cells and $CD4^+$ $CCR5^+$ A3.01.CCR5 cells, respectively, with non-pseudotyped or VSV-G-pseudotyped cell-free viruses. With the same amount of viral input, the original panel of NLCI viruses displayed a broad range of infectivity as described earlier, whereas all VSV-G pseudotyped viruses infected to similar levels

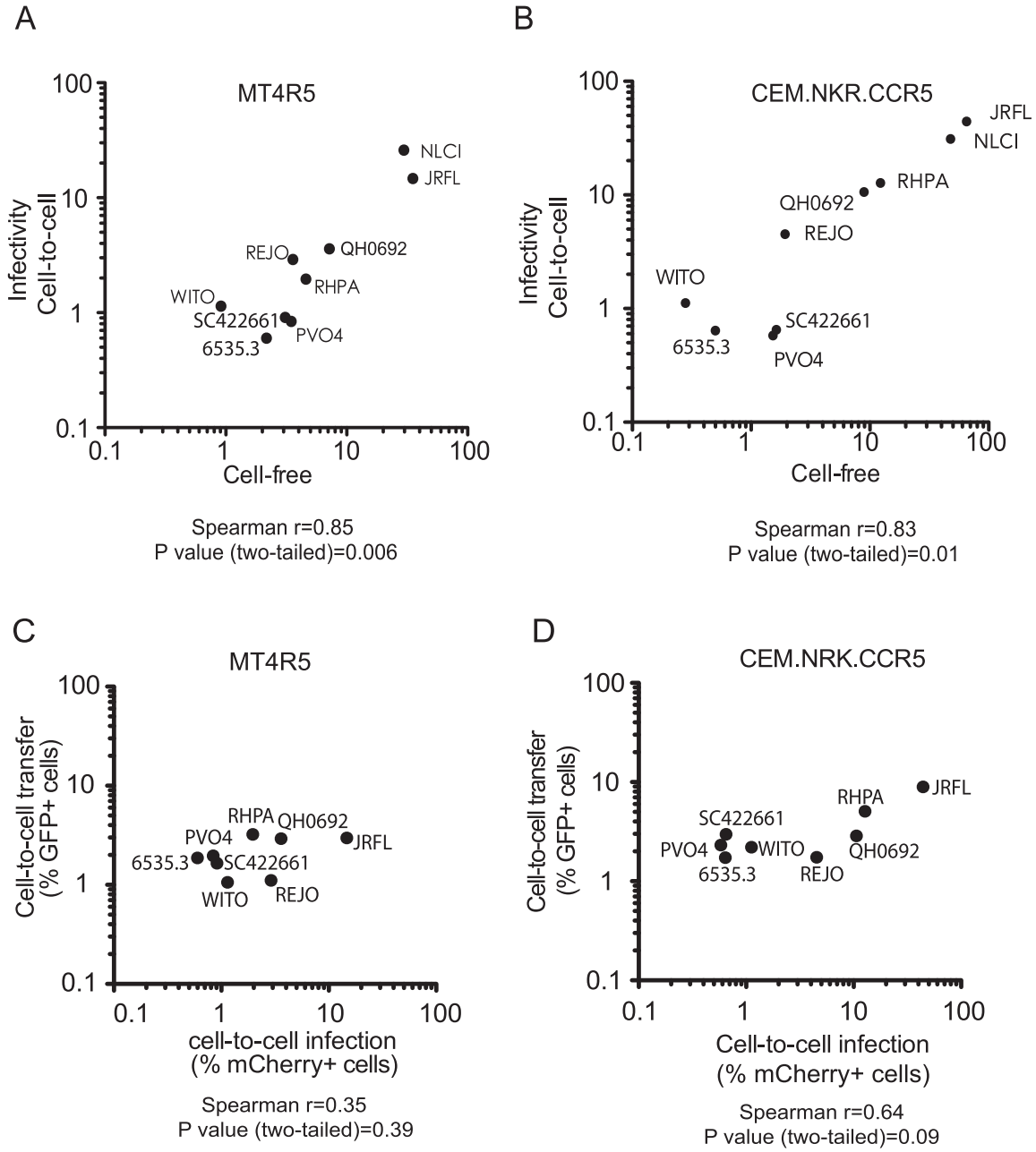

Fig. 6. Relative infection efficiency of cell-to-cell transmission correlated with that in cell-free infection while not with the efficiency of cell-to-cell transfer. The infection efficiencies of HIV-1 with different Envs in cell-to-cell transmission correlated with that in cell free infection (A) MT4R5 cells and (B) CEM.NKR.CCR5 cells. The infection efficiencies of HIV-1 with different Envs in cell-to-cell transmission were not correlated with the efficiency of cell-to-cell transfer in (C) MT4R5 cells and (D) CEM.NKR.CCR5 cells.

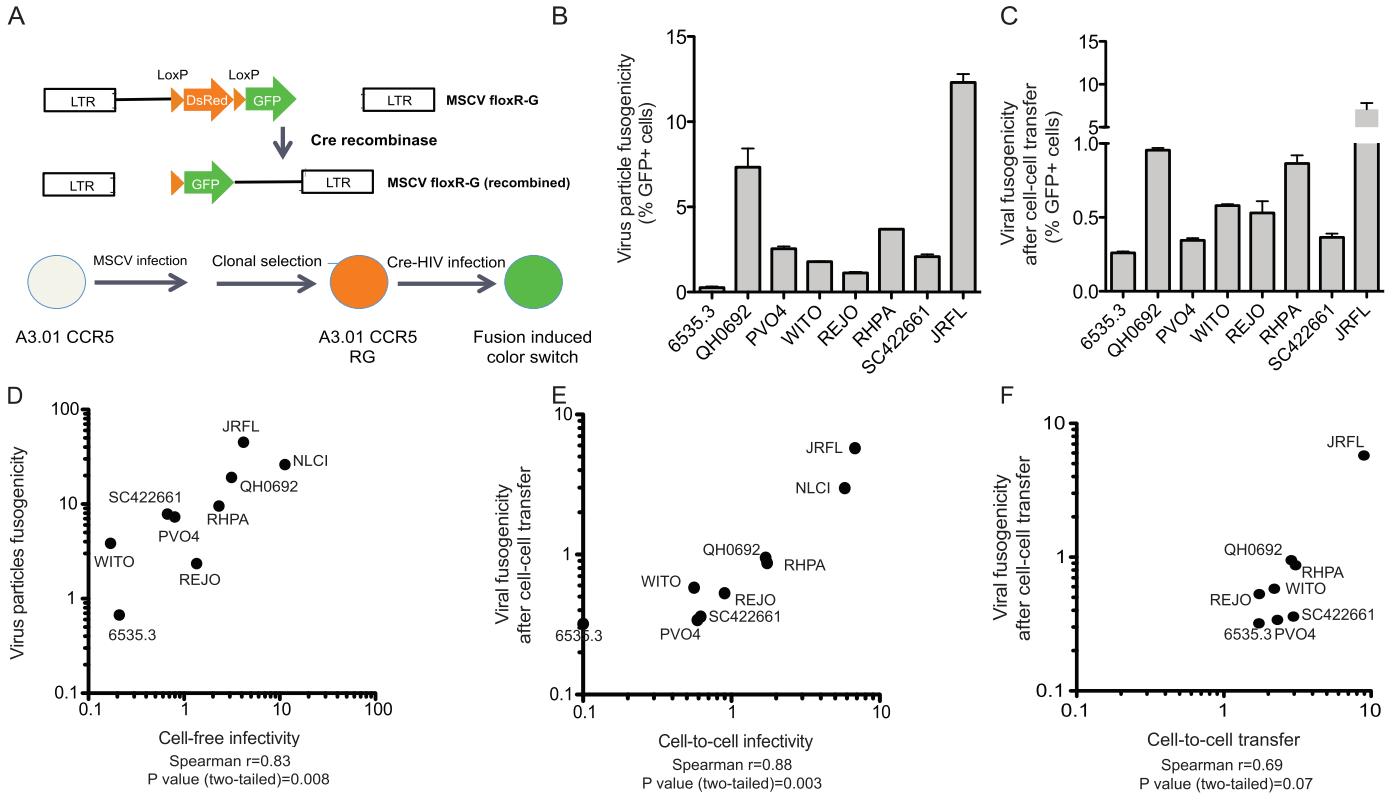

Fig. 7. Infectivity significantly correlated with Env fusogenicity in both modes of transmission. (A) A3.01.CCR5 RG cells were generated by transducing A3.01.CCR5 cells with MSCV floxR-G cassette that expresses dsRed and switched to GFP in response to Cre recombinase. Env fusogenicity was measured with in both cell-free virus particles (B) and cell-associated virus (C). The infection efficiencies of HIV-1 with different Envs in cell-free infection (D) and cell-to-cell infection (E) significantly correlated with the corresponding fusogenicity measured in A3.01.CCR5 RG cells in Cre-induced fusion assay, while not with the efficiency of cell-to-cell transfer (F). (For interpretation of the references to color in this figure legend, the reader is referred to the web version of this article.).

indicating that the infectivity differences are predominantly due to the *env* gene that is used (Fig. 8). These results suggested that weaker infectivity of viruses with T/F Envs may be attributed to the intrinsically low fusogenicity of the Env glycoprotein, again indicating that viral fusion, rather than the cell-to-cell transfer through VS, is the rate-limiting step during T/F virus infection, in both cell-free and cell-to-cell routes.

3. Discussion

Cell-to-cell infection between HIV-1 infected cells and uninfected CD4$^+$ T cells has been studied using different systems (Jolly et al., 2004; Reh et al., 2015; Oberle et al., 2016; Abela et al., 2012; Malbec et al., 2013; Gombos et al., 2015; Durham et al., 2012). Most previous studies of HIV-1 cell-free and cell-to-cell infection have utilized the lab-adapted HIV-1 strain NL4-3. Compared to lab-adapted viral strains, T/F viruses are less well characterized. Recent work on T/F viruses has sought to determine the properties that are selected for during newly acquired infection (Keele, 2010; Oberle et al., 2016; Wilen et al., 2011; Ochsenbauer et al., 2012; Lynch et al., 2011; Salazar-Gonzalez et al., 2009; Claiborne et al., 2015). As the only surface viral protein that mediates virus infection, as well as being the major target for cellular and humoral immune responses, HIV-1 Env is likely to possess important transmission-related properties that are discernable from chronic strains, such as resistance to IFN and IFN-induced trans-membrane proteins (IFITMs) (Iyer et al., 2017; Foster et al., 2016; Yu et al., 2015). Although disparate results have been reported as to the relative resistance of T/F against IFN compared to non-transmitted viruses (Deymier et al., 2015; Oberle et al., 2016), IFITMs have been reported to restrict HIV-1 infection in both cell-free as well as cell-to-cell infection to varying degrees by directly interacting with Env, inhibiting Env processing or incorporation (Foster et al., 2016; Yu et al., 2015).

In this study, we developed a panel of fluorescent protein-expressing infectious proviral molecular clones of HIV-1 that carry Clade B T/F Envs, enabling us to characterize and directly compare T/F viruses where the only genetic difference is the sequence that encodes the Env glycoprotein. We utilized a T cell-to-T cell transmission assay to study cell-free versus cell-to-cell infection efficiencies. We observed that the panel of viruses with T/F Envs displayed a wide range of infectivity in cell-free and cell-to-cell infection assays and were also less infectious when compared to lab strain $NLCI_{NL4-3}$ and chronic viral strain $NLCI_{JRFL}$ in single round infection assays using various different T cell lines (Fig. 3A and B) as well as in standard TZM-bl assays (Fig. 2A, B). The robust infectivity of the lab strain NL4-3, as well as chronic strain JRFL, may relate to its history of being extensively passaged *in vitro*. The panel of viruses with various T/F Envs also exhibited different levels of replication during multiple rounds of productive infection (Fig. 4) except for the 6535.3 Env, which did not replicate well in culture, perhaps due to its poor incorporation into viral particles (Fig. 1C, D).

A previous study of some of the same T/F Envs by Ochsenbauer et al. Ochsenbauer et al. (2012), found that T/F viruses, including RHPA, REJO and WITO, displayed similar replication kinetics in primary CD4$^+$ lymphocytes at day 10 after infection measured by p24 production. In the present study, however, we observed a significant range in replication efficiency among different T/F strains, as well as between T/F strains and lab-adapted / chronic strain as early as two days after infection.

To assess synapse formation and the transfer of virus during HIV-1 cell-to-cell infection (Dale et al., 2011), we measured the efficiency with which the T/F Envs could initiate transfer of HIV-1 from infected donor cells to uninfected target cells. Interestingly, although the panel of viruses with T/F Envs displayed a wide range of cell-to-cell infection

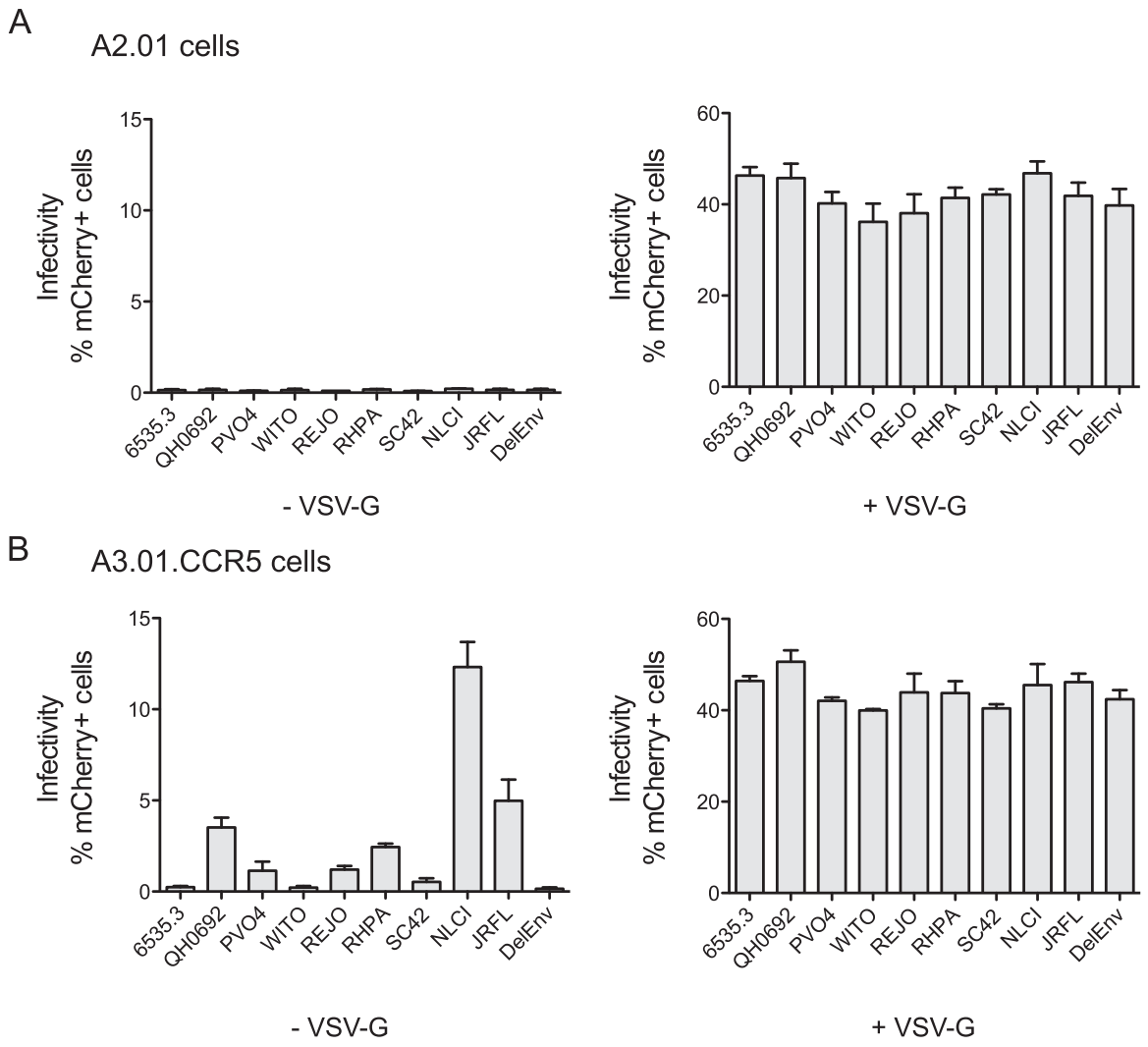

Fig. 8. Cell-free single round infectivity of VSV-G pseudotyped viruses in A2.01 and A3.01.CCR5 cells. Cell-free infection levels of A2.01 cells (A) and A3.01.CCR5 cells (B) by 5 ng/well of viruses with T/F Envs (left), compared to 5 ng/well of viruses pseudotyped with VSV-G (right). Error bars represent SEMs of duplicate wells from two independent experiments.

efficiencies, they were capable of similarly efficient cell-to-cell transfer into target cells (Fig. 5C, D). Even the least infectious clone with 6535.3 Env was able to mediate VS formation as well as viral transfer comparable to the more infectious clones, such as QH0692. We also note that the levels of cell-to-cell transfer of virus were surprisingly insensitive to the variable levels of Env surface expression. We observed that T/F Envs were expressed on the surface of infected donor cells at different levels, as shown by surface Env staining with mAb 2G12 (Fig. 5B), however, they all maintained the ability to engage in VS formation and subsequent cell-to-cell transfer. Taken together, these results suggest that Env expression levels may not be the rate-limiting factor in cell-to-cell transfer of HIV-1, and that cell-to-cell transfer is a conserved feature of T/F Env, independent of their infectivity *in vitro*.

Interestingly, we also observed that the relative infection efficiency in cell-free infection significantly correlated with that in cell-to-cell infection (Fig. 6A, B), while neither of them displayed significant correlation with the efficiency of cell-to-cell transfer (Fig. 6C, D). When fusogenicity of T/F Envs was measured using viral membrane fusion assay (Esposito et al., 2016), we found that they directly correlated with the viral infectivity (Fig. 7D, E). VSV-G pseudo-typing complemented the low fusogenicity of T/F Envs, and enabled the viruses to infect target cells with relatively comparable efficiency (Fig. 8). This suggests that low infectivity in cell-to-cell infection may be attributed to intrinsically low fusogenicity of T/F Envs.

We interpret these results within a context of a “two-step entry” model (Dale et al., 2011), where a viral transfer step precedes viral membrane fusion. Cell-to-cell infection requires that Envs expressed on the surface of infected cells maintain their ability to interact with CD4 and engage in VS formation to allow transfer of virus in a fusion-independent manner. While the T/F Env generally showed similar transfer efficiency, fusion potential of T/F Envs can exhibit greater variation. During cell-to-cell infection, once transferred virus particles are associated with target cells, they may be able to infect with different efficiency depending on fusogenic potentials of the different Envs.

We also observe that viruses with T/F Envs exhibited lower infectivity *in vitro* compared to lab-adapted strain such as NL4-3 or JRFL. Recent studies identified different conformational stages of mature unliganded Env trimers by assessing dynamics of Env using single molecule fluorescence resonance energy transfer (smFRET) (Munro et al., 2014). It has been observed that lab-adapted NL4-3 Env trimers tend to adopt an “open” conformation and spontaneously access high-energy states, which are associated with CD4 and co-receptor binding. However, greater proportions of Envs from primary isolates have been found to adopt a “closed” and much less dynamic ground state conformation (Munro et al., 2014; Ma et al., 2018), reducing the ability to interact with CD4 and co-receptors (Munro et al., 2014). The strain

from which lab-adapted clone NL4-3 was derived was extensively passaged in T cell lines without immune pressures (Adachi et al., 1986), and therefore may have undergone selection for greater fusogenicity and infectivity. The "closed" conformation of T/F Envs, on the other hand, may result from maintaining a balance of the ability to establish infection and to evade immune pressures during viral transmission *in vivo*. Based on this model and the results we presented here, we suggest that the lower infectivity of T/F viruses is due to their intrinsically low fusogenicity and may be associated with selection pressure such as IFN during the process of viral transmission (Iyer et al., 2017).

Viruses bearing various T/F Envs are similarly capable of efficient viral transfer from infected donor cells to uninfected target cells. We speculate that the conservation of cell-to-cell transfer by T/F Env is indicative of a biologically important function of Env. However, for both routes of viral transmission the intrinsic fusogenicity of T/F Envs determines viral infectivity. This dependency may be part of a cost-benefit evolution of the virus, and may allow for evasion of immune surveillance, or resistance to IFN and IFN-induced host factors such as IFITMs. Additional studies are required to determine the role it may play in acute HIV-1 infection.

4. Material and methods

4.1. Viral constructs

A panel of full-length Clade B primary isolate Transmitted/Founder (T/F) HIV-1 Env (ARP Cat #11227, Drs. David Montefiori and Beatrice Hahn) were cloned into pNL4-3 based $NLCI_{NL4-3}$ backbone in place of NL4-3 (Adachi et al., 1986) Env (Table 1). $NLCI_{NL4-3}$ is a proviral molecular clone with mCherry in the *nef* locus. Nef expression is restored by internal ribosome entry site (IRES) (Cohen et al., 1999). $NLCI_{JRFL}$ was generated using full-length JRFL Env, a chronic CCR5-tropic Env. Gag-iGFP and Gag-iCre, as previously described (Hubner et al., 2007; Esposito et al., 2016), have GFP or Cre inserted into Gag in frame between MA and CA domains. The same panel of *env* was also cloned into Gag-iGFP and Gag-iCre respectively, replacing NL4-3 *env*. All constructs were generated using overlap PCR with restriction enzymes EcoRI and MluI. PCR amplified sequences were verified by Sanger sequencing.

4.2. Cells and cell culture

Human cell lines Jurkat E6-1 and CEM.NKR-CCR5 were obtained from Dr. Arthur Weiss and Dr. Alexandra Trkola respectively from the NIH AIDS Reagent Program (ARP). Cells were maintained in RPMI 1640 medium containing 10% fetal bovine serum (FBS), 100 U/ml penicillin, 100 μg/ml streptomycin, and 2 mM glutamine (complete RPMI medium) and were passaged regularly and maintained at density of below 1×10^6/ml. MT4R5 cell line was obtained from Dr. James E. Robinson, and cultured in complete RPMI medium supplemented with 2 μg/ml puromycin. A3.01.CCR5 cell line was obtained from Dr. Robert McLinden from ARP. Propagation medium of these cells was complete RPMI supplemented with 1 mg/ml G418. A2.01 cells were obtained from Dr. Thomas Folks from APR, and were cultured in complete RPMI medium. Cell lines 293T and TZM-bl cell lines were obtained from ATCC and maintained in Dulbecco's Modified Eagle Medium (DMEM) containing 10% fetal bovine serum (FBS), 100 U/ml penicillin, 100 μg/ml streptomycin, and 2 mM glutamine. Primary $CD4^+$ T cells were obtained from human peripheral blood through the New York Blood Center and isolated by negative selection with a Miltenyi $CD4^+$ T cell isolation kit II (Miltenyi Biotec). Unactivated $CD4^+$ T cells were maintained in 10 U/ml interleukin (IL-2, ARP). Primary CD4+ T cells were activated by co-culturing with irradiated allogeneic peripheral blood mononuclear cells (PBMC) in complete RPMI medium with 100 U/ml IL2 and 2 μg/ml phytohemagglutinin (PHA) and used 2–3 days after activation. Stable cell line A3.01.CCR5 RG was generated by transduction with retrovirus MSCV containing a WPRE vector where dsRed was flanked by LoxP and followed by Cre-activated enhanced GFP (Esposito et al., 2016) (plasmid 32702; Addgene, Sadelain lab and Clevers lab).

4.3. p24 enzyme linked immunosorbent assay (ELISA)

P24 ELISA was performed following a modified version of a previously published protocol (Moore et al., 1990). Costar 3922 flat bottom high binding plates were pre-coated with 50 μg/ml (in 0.1 M $NaHCO_3$) anti-p24 capturing antibody (Aalto D7320) over night at room temperature. Coated plate was washed with 1x TBST, blocked with 2% nonfat milk (Lab Scientific) for 1 h and washed again in TBST. HIV-1-containing supernatant was lysed and serially diluted with 1% empigen, and added to treated plates. P24 standard of known concentration was serially diluted in the same solution and incubated in the same plate. After 3-h incubation at room temperature, the plate was washed 4 times with 0.05% Tris-buffered saline and Tween 20 (TBST) and incubated for 1 additional hour with 0.5 μg/ml alkaline phosphatase conjugated mouse anti-HIV p24 antibody (CLINIQA) in TBST with 20% sheep serum. After extensive washing with TBST, 50 ul of Sapphire Substrate (Tropix) was added into each well and incubated for 20 min before the luminescence was quantitated on Fluo Star Optima plate reader. Linear regression standard curve and sample analysis was performed using Prism (Graphpad software inc.).

4.4. Western Blot

Virus supernatant from transfected 293T cells was collected and quantitated by p24 ELISA. Virus was pelleted by ultracentrifugation through 6% Opti-prep density gradient medium (Sigma Aldrich) and resuspended in PBS and quantitated by p24 ELISA. Both of concentrated virus and transfected 293T cells were lysed with 1% Tris-Triton lysis buffer supplemented with 1x protease inhibitor (Roche). Lysed 293T cells were centrifuged at 13,000 rpm for 3 min at 4 °C. Total protein concentration in cell lysates was determined by Coomassie Plus assay kit (Thermo Scientific). Cell lysates and viral particle lysates were normalized according to protein concentration and p24 amount respectively. All samples were denatured and reduced before being separated by sodium dodecyl sulfate polyacrylamide gel electrophoresis (SDS-PAGE). Protein was transferred to Polyvinylidene difluoride (PVDF) membrane (GE Healthcare) for antibody detection. Polyclonal sheep anti-gp120 antibody (Dr. Micheal Phelan, ARP) was used to probe gp120 and gp160; Pooled Clade B HIV-1 infected patient IgG was used to probe all HIV-1 viral proteins (Dr. Luiz Barbosa, ARP). Horseradish peroxidase (HRP) conjugated anti-sheep or anti-human antibodies (Jackson ImmunoResearch Laboratories, Inc) were used as secondary antibodies. Chemiluminescence signal was detected by SuperSignal west Femto Maximum Sensitivity substrate (ThermoFisher Scientific) and visualized with FluorChem E imaging system (ProteinSimple). Signal intensity was quantitated with Image J (Wayne Rasband, National Institutes of Health).

4.5. Surface Tetherin staining

Nucleofection was used to transfect NLCI HIV-1 constructs in Tetherin high Jurkat cells (Alvarez et al., 2014) (Amaxa Biosystems). Viable cells were purified from transfected populations through ficoll paque (GE healthcare) density gradient purification 24 h post transfection. Anti-tetherin APC antibody (Biolegend) was used at concentration of 5 μg/ml in PBS with 2% FBS for 30 min at 4 °C. Cells were fixed with 2% paraformaldehyde prior to analysis by flow cytometry.

4.6. TZM-bl assay

Cell-free virus particles were produced by transfection of 293T cells using Polyjet (SignaGen) with NLCI based primary isolates plasmid

DNA. Cell-free virus particles were harvested 48 h after transfection of 293T cells, centrifuged at 1000*g*, filtered with membrane with pore size of 0.45 μm and stored in −80 °C freezer. Viral supernatant was quantified by p24 enzyme linked immunosorbent assay. 4.5 ng of viruses were used to infect 2×10^4 pre-seeded TZM-bl cells in flat bottom 96 well plates. HIV-1 virus-containing supernatant was added to each well and incubated for 48 h in the presence or absence of 30 μg/ml of DEAE-Dextran. 48 h post infection, TZM-bl cells were washed and lysed with cell culture lysis reagent (Promega) and 20 μl of each sample was read on Fluo Star Optima plate reader with injection of 100 μl of Luciferase Assay Reagent (Promega).

Cell-to-cell infection of TZM-bl cells was performed by overlaying 2×10^4 nucleofected Jurkat cells (described above) on top of the same number of pre-seeded TZM-bl cells in flat bottom 96 well plate in the presence or absence of 2 μg/ml DEAE-Dextran. 48 h after infection, samples were collected and read the same way as in the cell-free assay.

4.7. Single round cell-free infection assay in T cells

Cell-free virus particles were prepared as described above. Different viruses were normalized to the same input of p24 antigen. Virus containing 4.5 ng p24 was used infect 1.5×10^5 CCR5 expressing T cells in each well of flat bottom 96 well plates. 2 μg/ml of polybrene was present in the infection assay to facilitate cell-free infection. In the case of A3.01.CCR5 cells, 16 μg/ml of polybrene was used. To ensure measurement of a single round of infection, at 18 h post infection, medium was replaced with fresh medium containing 10uM azidothymidine (AZT; ARP). At 48 h post infection, cells were treated with tryspin-EDTA (Gibco) to remove surface-attached viral particles, neutralized with complete RPMI medium, washed with phosphate-buffered saline (PBS, Sigma) and fixed with 2% paraformaldehyde. mCherry fluorescence signal from infected cells were detected by flow cytometry using BD LSRFortessa flow cytometer (BD Biosciences) and analyzed with Flowjo (Tree Star, Inc).

4.8. Single round cell-to-cell infection assay in T cells

Cell-associated viral inoculum was provided by Jurkat cells nucleofected with the panel of NLCI constructs that carry primary isolate Envs. Nucleofected donor cells were cultured overnight, after which dead cells were removed by Ficoll paque (GE healthcare) density gradient centrifugation. Nucleofected donor Jurkat cells and target CCR5-expressing $CD4^+$ T cells were dye-labeled with 5uM cell proliferation dye eFluor 670 (eBiosciences) and 10 μM cell proliferation dye eFluor 450 (eBiosciences) respectively. At the time of co-culture, the percentage of HIV-expressing donor cells was adjusted to a similar fraction of all cells, by adjusting amount of DNA used in nucleofection or by diluting donor cells with non-nucleofected Jurkat cells. 1.5×10^5 donor cells were co-cultured with same number of HIV-1 naïve target cells in each well of round bottom 96 well plates. To measure single round infection, medium was replaced with fresh medium containing 10 uM AZT about 18 h after the co-culture. At 40–48 h post infection cells were treated with trypsin-EDTA to remove surface-attached viral particles and to disrupt donor-target doublets. Cells were then neutralized with complete RPMI medium, washed with PBS and fixed with 2% paraformaldehyde. Samples were then analyzed with LSR Fortessa flow cytometer (BD Biosciences) and the Flowjo software (Tree Star, inc). mCherry fluorescence signal from efluor450 labeled target population represent cells that were infected with HIV-1 through cell-to-cell transmission.

4.9. Surface Env mAb staining

Jurkat cells were nucleofected with T/F Envs carrying NLCI constructs as described previously in cell-to-cell infection assay. Viable cells were separated by ficoll gradient centrifugation, washed and placed into V bottom 96 well plate at density of 1.5×10^5 per well and stained with 10 μg/ml HIV-1 monoclonal antibody 2G12 at 4 °C for 45 min followed by 2 μg/ml Alexa Fluor (AF) 647 conjugated goat anti-human IgG (Life technologies) at 4 °C for 30 min. Samples were then washed and fixed for FACS. Average of median fluorescence intensity was calculated from two independent experiments.

To quantitate cell-surface Env expression level, we examined the mean fluorescence intensity (MFI) of mCherry high population, corresponding to HIV-1 infected cells that express both early and late HIV-1 genes, including Env. The level of surface Env binding by each anti-HIV mAb was calculated as relative MFI, which is a ratio of MFI of Env-AF647 over secondary antibody alone control.

Relative MFI = (MFI Env-AF647 - MFI secondary antibody control)/ MFI secondary antibody alone control.

4.10. Cell-to-cell transfer assay

Cell-associated viral inoculum was prepared by nucleofecting Jurkat cells with the panel of Gag-iGFP constructs that carry T/F Envs. Nucleofected donor Jurkat cells and target CCR5-expressing $CD4^+$ T cells were dye-labeled with cell proliferation dye eFluor 670 and eFluor 450 respectively. At the time of co-culture, the percentage of HIV-expressing donor cells was adjusted to a similar fraction of all cells, by adjusting amount of DNA used in nucleofection or by diluting donor cells with non-nucleofected Jurkat cells. 1.5×10^5 donor cells were co-cultured with same number of HIV-1 naïve target cells in each well of round bottom 96 well plates. 3 h after the co-culture, cells were treated with trypsin-EDTA to remove surface-attached viral particles and to disrupt donor-target doublets. Cells were then neutralized with complete RPMI medium, washed with PBS and fixed with 2% paraformaldehyde. Samples were then analyzed with LSRFortessa flow cytometer (BD Biosciences) and Flowjo (Tree Star, inc). GFP+ signal from efluor450 labeled target population represent cells that obtained viral transfer from HIV-1 expressing donor cells.

4.11. Multiple rounds of infection

To examine the ability of the viruses to undergo multi-rounds of infection, we initiated the infection with either cell-free viruses produced from transfected 293T cells (2.5 ng p24) or by nucleofected Jurkat cells as described in the single round cell-to-cell infection assay. Primary CD4+ T cells were isolated and activated as previously described, labeled with proliferative dye efluor450 and used as target cells in a multiround infection assay. We collected samples every two days and split cells to maintain optimal density. Samples were then analyzed with LSRFortessa flow cytometer (BD Biosciences) and Flowjo (Tree Star, inc). mCherry+ signal from efluor450 labeled target population represent cells infected with HIV-1.

4.12. Cell-free and cell-to-cell fusion assay

Cell-free virus particles that package Cre recombinase were produced by transfecting 293T cells and quantified using p24 ELISA. 4.5 ng of each different virus was used to infect 1.5×10^5 A3.01.CCR5 RG reporter cells in flat bottom 96 well plate format. After 40 h of incubation at 37 °C, cells were washed with PBS, trypsinized to remove surface-attached free virus particles, neutralized with complete RPMI medium, washed again with PBS and fixed with 2% paraformaldehyde for flow cytometry.

For measurement of fusion in cell-to-cell infection, Jurkat cells nucleofected with Gag-iCre constructs that carry different Clade B T/F Envs were used as donor cells, and prepared as previously described (Esposito et al., 2016). A3.01.CCR5 RG cells were used as target cells. The donor and target cells were labeled with cell proliferative dye eFluor670 and eFluor450 respectively. 1.5×10^5 donor cells and the same number of target cells were mixed in each well of round bottom

96-well plate. After a 40-h incubation at 37 °C, we collected samples as previously described for flow cytometry analysis. GFP + signal from eFluor450-labeled target population represent cells in which viral fusion events have occurred.

Acknowledgements

We would like to acknowledge funding from the following sources NIH/NIGMS GM113885, NIH/NIAID AI116191, and NIH/NIDA DA041765.

References

Abela, I.A., Berlinger, L., Schanz, M., Reynell, L., Gunthard, H.F., Rusert, P., Trkola, A., 2012. Cell-cell transmission enables HIV-1 to evade inhibition by potent CD4bs directed antibodies. PLoS Pathog. 8, e1002634.

Adachi, A., Gendelman, H.E., Koenig, S., Folks, T., Willey, R., Rabson, A., Martin, M.A., 1986. Production of acquired immunodeficiency syndrome-associated retrovirus in human and nonhuman cells transfected with an infectious molecular clone. J. Virol. 59, 284–291.

Alvarez, R.A., Hamlin, R.E., Monroe, A., Moldt, B., Hotta, M.T., Rodriguez Caprio, G., Fierer, D.S., Simon, V., Chen, B.K., 2014. HIV-1 Vpu antagonism of tetherin inhibits antibody-dependent cellular cytotoxic responses by natural killer cells. J. Virol. 88, 6031–6046.

Ashokkumar, M., Aralaguppe, S.G., Tripathy, S.P., Hanna, L.E., Neogi, U., 2018. Unique phenotypic characteristics of recently transmitted HIV-1 subtype C envelope glycoproteingp120: use of CXCR6 coreceptor by transmitted founder viruses. J. Virol. 92.

Back, N.K., Smit, L., De Jong, J.J., Keulen, W., Schutten, M., Goudsmit, J., Tersmette, M., 1994. An N-glycan within the human immunodeficiency virus type 1 gp120 V3 loop affects virus neutralization. Virology 199, 431–438.

Bernard-Stoecklin, S., Gommet, C., Cavarelli, M., Le Grand, R., 2014. Nonhuman primate models for cell-associated simian immunodeficiency virus transmission: the need to better understand the complexity of HIV mucosal transmission. J. Infect. Dis. 210 (Suppl. 3), S660–S666.

Bosch, B., Grigorov, B., Senserrich, J., Clotet, B., Darlix, J.L., Muriaux, D., Este, J.A., 2008. A clathrin-dynamin-dependent endocytic pathway for the uptake of HIV-1 by direct T cell-T cell transmission. Antivir. Res. 80, 185–193.

Brandenberg, O.F., Rusert, P., Magnus, C., Weber, J., Boni, J., Gunthard, H.F., Regoes, R.R., Trkola, A., 2014. Partial rescue of V1V2 mutant infectivity by HIV-1 cell-cell transmission supports the domain's exceptional capacity for sequence variation. Retrovirology 11, 75.

Cao, J., Sullivan, N., Desjardin, E., Parolin, C., Robinson, J., Wyatt, R., Sodroski, J., 1997. Replication and neutralization of human immunodeficiency virus type 1 lacking the V1 and V2 variable loops of the gp120 envelope glycoprotein. J. Virol. 71, 9808–9812.

Checkley, M.A., Luttge, B.G., Freed, E.O., 2011. HIV-1 envelope glycoprotein biosynthesis, trafficking, and incorporation. J. Mol. Biol. 410, 582–608.

Chen, B.K., 2012. T cell virological synapses and HIV-1 pathogenesis. Immunol. Res. 54, 133–139.

Chen, P., Hubner, W., Spinelli, M.A., Chen, B.K., 2007. Predominant mode of human immunodeficiency virus transfer between T cells is mediated by sustained Env-dependent neutralization-resistant virological synapses. J. Virol. 81, 12582–12595.

Chikere, K., Webb, N.E., Chou, T., Borm, K., Sterjovski, J., Gorry, P.R., Lee, B., 2014. Distinct HIV-1 entry phenotypes are associated with transmission, subtype specificity, and resistance to broadly neutralizing antibodies. Retrovirology 11, 48.

Chohan, B., Lang, D., Sagar, M., Korber, B., Lavreys, L., Richardson, B., Overbaugh, J., 2005. Selection for human immunodeficiency virus type 1 envelope glycosylation variants with shorter V1-V2 loop sequences occurs during transmission of certain genetic subtypes and may impact viral RNA levels. J. Virol. 79, 6528–6531.

Claiborne, D.T., Prince, J.L., Scully, E., Macharia, G., Micci, L., Lawson, B., Kopycinski, J., Deymier, M.J., Vanderford, T.H., Nganou-Makamdop, K., Ende, Z., Brooks, K., Tang, J., Yu, T., Lakhi, S., Kilembe, W., Silvestri, G., Douek, D., Goepfert, P.A., Price, M.A., Allen, S.A., Paiardini, M., Altfeld, M., Gilmour, J., Hunter, E., 2015. Replicative fitness of transmitted HIV-1 drives acute immune activation, proviral load in memory CD4+ T cells, and disease progression. Proc. Natl. Acad. Sci. USA 112, E1480–E1489.

Cohen, G.B., Gandhi, R.T., Davis, D.M., Mandelboim, O., Chen, B.K., Strominger, J.L., Baltimore, D., 1999. The selective downregulation of class I major histocompatibility complex proteins by HIV-1 protects HIV-infected cells from NK cells. Immunity 10, 661–671.

Dale, B.M., McNerney, G.P., Thompson, D.L., Hubner, W., de Los Reyes, K., Chuang, F.Y., Huser, T., Chen, B.K., 2011. Cell-to-cell transfer of HIV-1 via virological synapses leads to endosomal virion maturation that activates viral membrane fusion. Cell Host Microbe 10, 551–562.

Derdeyn, C.A., Decker, J.M., Bibollet-Ruche, F., Mokili, J.L., Muldoon, M., Denham, S.A., Heil, M.L., Kasolo, F., Musonda, R., Hahn, B.H., Shaw, G.M., Korber, B.T., Allen, S., Hunter, E., 2004. Envelope-constrained neutralization-sensitive HIV-1 after heterosexual transmission. Science 303, 2019–2022.

Deymier, M.J., Ende, Z., Fenton-May, A.E., Dilernia, D.A., Kilembe, W., Allen, S.A., Borrow, P., Hunter, E., 2015. Heterosexual transmission of subtype C HIV-1 selects consensus-like variants without increased replicative capacity or interferon-alpha resistance. PLoS Pathog. 11, e1005154.

Durham, N.D., Chen, B.K., 2016. Measuring T cell-to-T cell HIV-1 transfer, viral fusion, and infection using flow cytometry. Methods Mol. Biol. 1354, 21–38.

Durham, N.D., Yewdall, A.W., Chen, P., Lee, R., Zony, C., Robinson, J.E., Chen, B.K., 2012. Neutralization resistance of virological synapse-mediated HIV-1 Infection is regulated by the gp41 cytoplasmic tail. J. Virol. 86, 7484–7495.

Esposito, A.M., Cheung, P., Swartz, T.H., Li, H., Tsibane, T., Durham, N.D., Basler, C.F., Felsenfeld, D.P., Chen, B.K., 2016. A high throughput Cre-lox activated viral membrane fusion assay identifies pharmacological inhibitors of HIV entry. Virology 490, 6–16.

Fenton-May, A.E., Dibben, O., Emmerich, T., Ding, H., Pfafferott, K., Aasa-Chapman, M.M., Pellegrino, P., Williams, I., Cohen, M.S., Gao, F., Shaw, G.M., Hahn, B.H., Ochsenbauer, C., Kappes, J.C., Borrow, P., 2013. Relative resistance of HIV-1 founder viruses to control by interferon-alpha. Retrovirology 10, 146.

Fiebig, E.W., Wright, D.J., Rawal, B.D., Garrett, P.E., Schumacher, R.T., Peddada, L., Heldebrant, C., Smith, R., Conrad, A., Kleinman, S.H., Busch, M.P., 2003. Dynamics of HIV viremia and antibody seroconversion in plasma donors: implications for diagnosis and staging of primary HIV infection. AIDS 17, 1871–1879.

Foster, T.L., Wilson, H., Iyer, S.S., Coss, K., Doores, K., Smith, S., Kellam, P., Finzi, A., Borrow, P., Hahn, B.H., Neil, S.J.D., 2016. Resistance of Transmitted founder HIV-1 to IFITM-mediated restriction. Cell Host Microbe 20, 429–442.

Freed, E.O., Martin, M.A., 1995. The role of human immunodeficiency virus type 1 envelope glycoproteins in virus infection. J. Biol. Chem. 270, 23883–23886.

Frost, S.D., Liu, Y., Pond, S.L., Chappey, C., Wrin, T., Petropoulos, C.J., Little, S.J., Richman, D.D., 2005. Characterization of human immunodeficiency virus type 1 (HIV-1) envelope variation and neutralizing antibody responses during transmission of HIV-1 subtype B. J. Virol. 79, 6523–6527.

Go, E.P., Hewawasam, G., Liao, H.X., Chen, H., Ping, L.H., Anderson, J.A., Hua, D.C., Haynes, B.F., Desaire, H., 2011. Characterization of glycosylation profiles of HIV-1 transmitted/founder envelopes by mass spectrometry. J. Virol. 85, 8270–8284.

Gombos, R.B., Kolodkin-Gal, D., Eslamizar, L., Owuor, J.O., Mazzola, E., Gonzalez, A.M., Korioth-Schmitz, B., Gelman, R.S., Montefiori, D.C., Haynes, B.F., Schmitz, J.E., 2015. Inhibitory effect of individual or combinations of broadly neutralizing antibodies and antiviral reagents against cell-free and cell-to-cell HIV-1 transmission. J. Virol. 89, 7813–7828.

Hallenberger, S., Bosch, V., Angliker, H., Shaw, E., Klenk, H.D., Garten, W., 1992. Inhibition of furin-mediated cleavage activation of HIV-1 glycoprotein gp160. Nature 360, 358–361.

Hraber, P., Korber, B.T., Lapedes, A.S., Bailer, R.T., Seaman, M.S., Gao, H., Greene, K.M., McCutchan, F., Williamson, C., Kim, J.H., Tovanabutra, S., Hahn, B.H., Swanstrom, R., Thomson, M.M., Gao, F., Harris, L., Giorgi, E., Hengartner, N., Bhattacharya, T., Mascola, J.R., Montefiori, D.C., 2014. Impact of clade, geography, and age of the epidemic on HIV-1 neutralization by antibodies. J. Virol. 88, 12623–12643.

Hubner, W., Chen, P., Del Portillo, A., Liu, Y., Gordon, R.E., Chen, B.K., 2007. Sequence of human immunodeficiency virus type 1 (HIV-1) Gag localization and oligomerization monitored with live confocal imaging of a replication-competent, fluorescently tagged HIV-1. J. Virol. 81, 12596–12607.

Hubner, W., McNerney, G.P., Chen, P., Dale, B.M., Gordon, R.E., Chuang, F.Y., Li, X.D., Asmuth, D.M., Huser, T., Chen, B.K., 2009. Quantitative 3D video microscopy of HIV transfer across T cell virological synapses. Science 323, 1743–1747.

Hunter, E., Swanstrom, R., 1990. Retrovirus envelope glycoproteins. Curr. Top. Microbiol. Immunol. 157, 187–253.

Iyer, S.S., Bibollet-Ruche, F., Sherrill-Mix, S., Learn, G.H., Plenderleith, L., Smith, A.G., Barbian, H.J., Russell, R.M., Gondim, M.V., Bahari, C.Y., Shaw, C.M., Li, Y., Decker, T., Haynes, B.F., Shaw, G.M., Sharp, P.M., Borrow, P., Hahn, B.H., 2017. Resistance to type 1 interferons is a major determinant of HIV-1 transmission fitness. Proc. Natl. Acad. Sci. USA 114, E590–E599.

Jolly, C., Sattentau, Q.J., 2004. Retroviral spread by induction of virological synapses. Traffic 5, 643–650.

Jolly, C., Kashefi, K., Hollinshead, M., Sattentau, Q.J., 2004. HIV-1 cell to cell transfer across an Env-induced, actin-dependent synapse. J. Exp. Med. 199, 283–293.

Jolly, C., Mitar, I., Sattentau, Q.J., 2007. Adhesion molecule interactions facilitate human immunodeficiency virus type 1-induced virological synapse formation between T cells. J. Virol. 81, 13916–13921.

Keele, B.F., 2010. Identifying and characterizing recently transmitted viruses. Curr. Opin. HIV AIDS 5, 327–334.

Keele, B.F., Derdeyn, C.A., 2009. Genetic and antigenic features of the transmitted virus. Curr. Opin. HIV AIDS 4, 352–357.

Keele, B.F., Giorgi, E.E., Salazar-Gonzalez, J.F., Decker, J.M., Pham, K.T., Salazar, M.G., Sun, C., Grayson, T., Wang, S., Li, H., Wei, X., Jiang, C., Kirchherr, J.L., Gao, F., Anderson, J.A., Ping, L.H., Swanstrom, R., Tomaras, G.D., Blattner, W.A., Goepfert, P.A., Kilby, J.M., Saag, M.S., Delwart, E.L., Busch, M.P., Cohen, M.S., Montefiori, D.C., Haynes, B.F., Gaschen, B., Athreya, G.S., Lee, H.Y., Wood, N., Seoighe, C., Perelson, A.S., Bhattacharya, T., Korber, B.T., Hahn, B.H., Shaw, G.M., 2008. Identification and characterization of transmitted and early founder virus envelopes in primary HIV-1 infection. Proc. Natl. Acad. Sci. USA 105, 7552–7557.

Koch, M., Pancera, M., Kwong, P.D., Kolchinsky, P., Grundner, C., Wang, L., Hendrickson, W.A., Sodroski, J., Wyatt, R., 2003. Structure-based, targeted deglycosylation of HIV-1 gp120 and effects on neutralization sensitivity and antibody recognition. Virology 313, 387–400.

Kolodkin-Gal, D., Hulot, S.L., Korioth-Schmitz, B., Gombos, R.B., Zheng, Y., Owuor, J., Lifton, M.A., Ayeni, C., Najarian, R.M., Yeh, W.W., Asmal, M., Zamir, G., Letvin, N.L., 2013. Efficiency of cell-free and cell-associated virus in mucosal transmission of human immunodeficiency virus type 1 and simian immunodeficiency virus. J. Virol. 87, 13589–13597.

Konopka, K., Stamatatos, L., Larsen, C.E., Davis, B.R., Duzgunes, N., 1991. Enhancement of human immunodeficiency virus type 1 infection by cationic liposomes: the role of CD4, serum and liposome-cell interactions. J. Gen. Virol. 72 (Pt 11), 2685–2696.

Law, K.M., Komarova, N.L., Yewdall, A.W., Lee, R.K., Herrera, O.L., Wodarz, D., Chen, B.K., 2016. In vivo HIV-1 cell-to-cell transmission promotes multicopy micro-compartmentalized infection. Cell Rep. 15, 2771–2783.
Learn, G.H., Muthui, D., Brodie, S.J., Zhu, T., Diem, K., Mullins, J.I., Corey, L., 2002. Virus population homogenization following acute human immunodeficiency virus type 1 infection. J. Virol. 76, 11953–11959.
Li, H., Zony, C., Chen, P., Chen, B.K., 2017. Reduced potency and incomplete neutralization of broadly neutralizing antibodies against cell-to-cell transmission of HIV-1 with transmitted founder Envs. J. Virol. 91.
Li, M., Salazar-Gonzalez, J.F., Derdeyn, C.A., Morris, L., Williamson, C., Robinson, J.E., Decker, J.M., Li, Y., Salazar, M.G., Polonis, V.R., Mlisana, K., Karim, S.A., Hong, K., Greene, K.M., Bilska, M., Zhou, J., Allen, S., Chomba, E., Mulenga, J., Vwalika, C., Gao, F., Zhang, M., Korber, B.T., Hunter, E., Hahn, B.H., Montefiori, D.C., 2006. Genetic and neutralization properties of subtype C human immunodeficiency virus type 1 molecular env clones from acute and early heterosexually acquired infections in Southern Africa. J. Virol. 80, 11776–11790.
Liu, Y., Curlin, M.E., Diem, K., Zhao, H., Ghosh, A.K., Zhu, H., Woodward, A.S., Maenza, J., Stevens, C.E., Stekler, J., Collier, A.C., Genowati, I., Deng, W., Zioni, R., Corey, L., Zhu, T., Mullins, J.I., 2008. Env length and N-linked glycosylation following transmission of human immunodeficiency virus Type 1 subtype B viruses. Virology 374, 229–233.
Ly, A., Stamatatos, L., 2000. V2 loop glycosylation of the human immunodeficiency virus type 1 SF162 envelope facilitates interaction of this protein with CD4 and CCR5 receptors and protects the virus from neutralization by anti-V3 loop and anti-CD4 binding site antibodies. J. Virol. 74, 6769–6776.
Lynch, R.M., Rong, R., Boliar, S., Sethi, A., Li, B., Mulenga, J., Allen, S., Robinson, J.E., Gnanakaran, S., Derdeyn, C.A., 2011. The B cell response is redundant and highly focused on V1V2 during early subtype C infection in a Zambian seroconverter. J. Virol. 85, 905–915.
Ma, X., Lu, M., Gorman, J., Terry, D.S., Hong, X., Zhou, Z., Zhao, H., Altman, R.B., Arthos, J., Blanchard, S.C., Kwong, P.D., Munro, J.B., Mothes, W., 2018. HIV-1 Env trimer opens through an asymmetric intermediate in which individual protomers adopt distinct conformations. Elife 7.
Malbec, M., Porrot, F., Rua, R., Horwitz, J., Klein, F., Halper-Stromberg, A., Scheid, J.F., Eden, C., Mouquet, H., Nussenzweig, M.C., Schwartz, O., 2013. Broadly neutralizing antibodies that inhibit HIV-1 cell to cell transmission. J. Exp. Med. 210, 2813–2821.
McCaffrey, R.A., Saunders, C., Hensel, M., Stamatatos, L., 2004. N-linked glycosylation of the V3 loop and the immunologically silent face of gp120 protects human immunodeficiency virus type 1 SF162 from neutralization by anti-gp120 and anti-gp41 antibodies. J. Virol. 78, 3279–3295.
Moore, J.P., McKeating, J.A., Weiss, R.A., Sattentau, Q.J., 1990. Dissociation of gp120 from HIV-1 virions induced by soluble CD4. Science 250, 1139–1142.
Munro, J.B., Gorman, J., Ma, X., Zhou, Z., Arthos, J., Burton, D.R., Koff, W.C., Courter, J.R., Smith 3rd, A.B., Kwong, P.D., Blanchard, S.C., Mothes, W., 2014. Conformational dynamics of single HIV-1 envelope trimers on the surface of native virions. Science 346, 759–763.
Murooka, T.T., Deruaz, M., Marangoni, F., Vrbanac, V.D., Seung, E., von Andrian, U.H., Tager, A.M., Luster, A.D., Mempel, T.R., 2012. HIV-infected T cells are migratory vehicles for viral dissemination. Nature 490, 283–287.
Oberle, C.S., Joos, B., Rusert, P., Campbell, N.K., Beauparlant, D., Kuster, H., Weber, J., Schenkel, C.D., Scherrer, A.U., Magnus, C., Kouyos, R., Rieder, P., Niederost, B., Braun, D.L., Pavlovic, J., Boni, J., Yerly, S., Klimkait, T., Aubert, V., Trkola, A., Metzner, K.J., Gunthard, H.F., Swiss, H.I.V.C.S., 2016. Tracing HIV-1 transmission: envelope traits of HIV-1 transmitter and recipient pairs. Retrovirology 13, 62.
Ochsenbauer, C., Edmonds, T.G., Ding, H., Keele, B.F., Decker, J., Salazar, M.G., Salazar-Gonzalez, J.F., Shattock, R., Haynes, B.F., Shaw, G.M., Hahn, B.H., Kappes, J.C., 2012. Generation of transmitted/founder HIV-1 infectious molecular clones and characterization of their replication capacity in CD4 T lymphocytes and monocyte-derived macrophages. J. Virol. 86, 2715–2728.
Parker, Z.F., Iyer, S.S., Wilen, C.B., Parrish, N.F., Chikere, K.C., Lee, F.H., Didigu, C.A., Berro, R., Klasse, P.J., Lee, B., Moore, J.P., Shaw, G.M., Hahn, B.H., Doms, R.W., 2013. Transmitted/founder and chronic HIV-1 envelope proteins are distinguished by differential utilization of CCR5. J. Virol. 87, 2401–2411.
Parrish, N.F., Gao, F., Li, H., Giorgi, E.E., Barbian, H.J., Parrish, E.H., Zajic, L., Iyer, S.S., Decker, J.M., Kumar, A., Hora, B., Berg, A., Cai, F., Hopper, J., Denny, T.N., Ding, H., Ochsenbauer, C., Kappes, J.C., Galimidi, R.P., West Jr., A.P., Bjorkman, P.J., Wilen, C.B., Doms, R.W., O'Brien, M., Bhardwaj, N., Borrow, P., Haynes, B.F., Muldoon, M., Theiler, J.P., Korber, B., Shaw, G.M., Hahn, B.H., 2013. Phenotypic properties of transmitted founder HIV-1. Proc. Natl. Acad. Sci. USA 110, 6626–6633.
Ping, L.H., Joseph, S.B., Anderson, J.A., Abrahams, M.R., Salazar-Gonzalez, J.F., Kincer, L.P., Treurnicht, F.K., Arney, L., Ojeda, S., Zhang, M., Keys, J., Potter, E.L., Chu, H., Moore, P., Salazar, M.G., Iyer, S., Jabara, C., Kirchherr, J., Mapanje, C., Ngandu, N., Seoighe, C., Hoffman, I., Gao, F., Tang, Y., Labranche, C., Lee, B., Saville, A., Vermeulen, M., Fiscus, S., Morris, L., Karim, S.A., Haynes, B.F., Shaw, G.M., Korber, B.T., Hahn, B.H., Cohen, M.S., Montefiori, D., Williamson, C., Swanstrom, R., Study, C.A.I., the Center for HIVAVIC, 2013. Comparison of viral Env proteins from acute and chronic infections with subtype C human immunodeficiency virus type 1 identifies differences in glycosylation and CCR5 utilization and suggests a new strategy for immunogen design. J. Virol. 87, 7218–7233.
Reh, L., Magnus, C., Schanz, M., Weber, J., Uhr, T., Rusert, P., Trkola, A., 2015. Capacity of broadly neutralizing antibodies to inhibit HIV-1 cell-cell transmission is strain- and epitope-dependent. PLoS Pathog. 11, e1004966.
Reitter, J.N., Means, R.E., Desrosiers, R.C., 1998. A role for carbohydrates in immune evasion in AIDS. Nat. Med. 4, 679–684.
Salazar-Gonzalez, J.F., Bailes, E., Pham, K.T., Salazar, M.G., Guffey, M.B., Keele, B.F., Derdeyn, C.A., Farmer, P., Hunter, E., Allen, S., Manigart, O., Mulenga, J., Anderson, J.A., Swanstrom, R., Haynes, B.F., Athreya, G.S., Korber, B.T., Sharp, P.M., Shaw, G.M., Hahn, B.H., 2008. Deciphering human immunodeficiency virus type 1 transmission and early envelope diversification by single-genome amplification and sequencing. J. Virol. 82, 3952–3970.
Salazar-Gonzalez, J.F., Salazar, M.G., Keele, B.F., Learn, G.H., Giorgi, E.E., Li, H., Decker, J.M., Wang, S., Baalwa, J., Kraus, M.H., Parrish, N.F., Shaw, K.S., Guffey, M.B., Bar, K.J., Davis, K.L., Ochsenbauer-Jambor, C., Kappes, J.C., Saag, M.S., Cohen, M.S., Mulenga, J., Derdeyn, C.A., Allen, S., Hunter, E., Markowitz, M., Hraber, P., Perelson, A.S., Bhattacharya, T., Haynes, B.F., Korber, B.T., Hahn, B.H., Shaw, G.M., 2009. Genetic identity, biological phenotype, and evolutionary pathways of transmitted/founder viruses in acute and early HIV-1 infection. J. Exp. Med. 206, 1273–1289.
Seaman, M.S., Janes, H., Hawkins, N., Grandpre, L.E., Devoy, C., Giri, A., Coffey, R.T., Harris, L., Wood, B., Daniels, M.G., Bhattacharya, T., Lapedes, A., Polonis, V.R., McCutchan, F.E., Gilbert, P.B., Self, S.G., Korber, B.T., Montefiori, D.C., Mascola, J.R., 2010. Tiered categorization of a diverse panel of HIV-1 Env pseudoviruses for assessment of neutralizing antibodies. J. Virol. 84, 1439–1452.
Sigal, A., Kim, J.T., Balazs, A.B., Dekel, E., Mayo, A., Milo, R., Baltimore, D., 2011. Cell-to-cell spread of HIV permits ongoing replication despite antiretroviral therapy. Nature 477, 95–98.
Sloan, R.D., Kuhl, B.D., Mesplede, T., Munch, J., Donahue, D.A., Wainberg, M.A., 2013. Productive entry of HIV-1 during cell-to-cell transmission via dynamin-dependent endocytosis. J. Virol. 87, 8110–8123.
Sourisseau, M., Sol-Foulon, N., Porrot, F., Blanchet, F., Schwartz, O., 2007. Inefficient human immunodeficiency virus replication in mobile lymphocytes. J. Virol. 81, 1000–1012.
Stamatatos, L., Cheng-Mayer, C., 1998. An envelope modification that renders a primary, neutralization-resistant clade B human immunodeficiency virus type 1 isolate highly susceptible to neutralization by sera from other clades. J. Virol. 72, 7840–7845.
Titanji, B.K., Aasa-Chapman, M., Pillay, D., Jolly, C., 2013. Protease inhibitors effectively block cell-to-cell spread of HIV-1 between T cells. Retrovirology 10, 161.
Wang, Y., Pan, Q., Ding, S., Wang, Z., Yu, J., Finzi, A., Liu, S.L., Liang, C., 2017. The V3 loop of HIV-1 Env determines viral susceptibility to IFITM3 impairment of viral infectivity. J. Virol. 91.
Wilen, C.B., Parrish, N.F., Pfaff, J.M., Decker, J.M., Henning, E.A., Haim, H., Petersen, J.E., Wojcechowskyj, J.A., Sodroski, J., Haynes, B.F., Montefiori, D.C., Tilton, J.C., Shaw, G.M., Hahn, B.H., Doms, R.W., 2011. Phenotypic and immunologic comparison of clade B transmitted/founder and chronic HIV-1 envelope glycoproteins. J. Virol. 85, 8514–8527.
Wyatt, R., Sodroski, J., 1998. The HIV-1 envelope glycoproteins: fusogens, antigens, and immunogens. Science 280, 1884–1888.
Yu, J., Li, M., Wilkins, J., Ding, S., Swartz, T.H., Esposito, A.M., Zheng, Y.M., Freed, E.O., Liang, C., Chen, B.K., Liu, S.L., 2015. IFITM proteins restrict HIV-1 infection by antagonizing the envelope glycoprotein. Cell Rep. 13, 145–156.